M 2015

U. PORTO

FEUP **FACULDADE DE ENGENHARIA**
UNIVERSIDADE DO PORTO

NANOPARTICLES AS NANOCARRIERS OF RESVERATROL FOR ALZHEIMER'S DISEASE

STÉPHANIE MACHADO ANDRADE
DISSERTAÇÃO DE MESTRADO APRESENTADA
À FACULDADE DE ENGENHARIA DA UNIVERSIDADE DO PORTO EM
ENGENHARIA BIOMÉDICA

Faculty of Engineering of University of Porto

U.PORTO

FEUP **FACULDADE DE ENGENHARIA**
UNIVERSIDADE DO PORTO

Nanoparticles as nanocarriers of resveratrol

for Alzheimer's disease

Stéphanie Machado Andrade

Dissertation carried out in the
Master in Biomedical Engineering

Supervisor: Prof. Dr. Maria do Carmo Pereira
Co-supervisor: Dr. Joana Angélica Loureiro

MEB – MESTRADO EM ENGENHARIA BIOMÉDICA   2014/2015

A Dissertação intitulada

"Nanoparticles as Nanocarriers of Resveratrol for Alzheimer's Disease"

foi aprovada em provas realizadas em 13-07-2015

o júri

Presidente Professor Doutor José Alberto Peixoto Machado da Silva
Professor Associado do Departamento de Engenharia Eletrotécnica e de
Computadores da Faculdade de Engenharia da U. Porto

Professora Doutora Maria Benedita Almeida Garrett de Sampaio Maia
Professora Auxiliar da Faculdade de Medicina Dentária da U. Porto

Professora Doutora Maria do Carmo da Silva Pereira
Professora Auxiliar do Departamento de Engenharia Química da Faculdade de
Engenharia da U. Porto

O autor declara que a presente dissertação (ou relatório de projeto) é da sua
exclusiva autoria e foi escrita sem qualquer apoio externo não explicitamente
autorizado. Os resultados, ideias, parágrafos, ou outros extratos tomados de ou
inspirados em trabalhos de outros autores, e demais referências bibliográficas
usadas, são corretamente citados.

Stephanie Machado Andrade
Autor – Stephanie Machado Andrade

Faculdade de Engenharia da Universidade do Porto

Resumo

Resveratrol (RES) tem sido descrito como agente terapêutico para a doença de Alzheimer (AD). Dadas as suas diversas vantagens do RES, acredita-se que é útil na terapia da AD. O RES apresenta baixa biodisponibilidade, resultante da sua baixa solubilidade em água e rápida depuração da circulação torna difícil estabelecer concentrações bioeficazes de RES no sangue e tecidos de seres humanos. Portanto, novas estratégias terapêuticas como sistemas de entrega de drogas específicas devem ser desenvolvidas a fim de superar essas limitações. Neste trabalho, RES e extratos de grainha e pele de uva foram encapsulados em lipossomas e nanopartículas de poli(ácido lático-co-ácido glicólico) (PLGA). Os lipossomas e as nanopartículas de PLGA com tamanhos e propriedades controlados foram preparados utilizando o método de hidratação de um fino filme lipídico e evaporação e emulsificação do solvente, respetivamente. Não foram obtidos valores significativos de eficiência de encapsulação para os lipossomas. As nanopartículas de PLGA preparadas apresentam uma forma esférica com diâmetros entre 158-182 nm, baixos valores de PdI e valores de potencial zeta negativos. Enquanto os valores de eficiência de encapsulação do RES encapsulado nas nanopartículas de PLGA foram cerca de 80±6%, para os extratos de grainha e pele de uva os valores de eficiência de encapsulação obtidos foram ligeiramente inferiores, 75±5% e 74±8%, respetivamente. O sistema preparado é estável em condições de armazenamento durante um mês. Os resultados dos ensaios de ThT e TEM demonstraram que os fármacos utilizados inibiram a formação das fibras $A\beta_{(1-42)}$. Os extratos têm um efeito inibitório mais pronunciado em comparação com o RES. Com 40 µM, RES inibe cerca de 86% da agregação do péptido, o extrato de pele de uva inibe cerca de 92% e o extrato de grainha de uva inibe cerca de 97%. À concentração de 80 µM, estes valores aumentaram para 91, 97 e 98%, respetivamente. Estes resultados sugerem que, para além de conter RES que inibe a agregação de $A\beta_{(1-42)}$, os extratos têm outros polifenóis que tornam este efeito inibidor mais pronunciado. Os estudos revelaram que as nanopartículas de PLGA carregadas com os fármacos usados também inibiram a formação de fibras de $A\beta_{(1-42)}$. À concentração de 40 µM, o RES encapsulado nas nanopartículas de PLGA inibiu cerca de 46% da agregação do péptido, o extrato de pele de uva encapsulado nas nanopartículas de PLGA inibiu cerca de 52% e o extrato de grainha de uva encapsulado nas nanopartículas de

PLGA inibiu cerca de 56%, depois 10 dias de incubação. A partir dos resultados obtidos, foi possível concluir que as nanopartículas de PLGA são um nanotransportador adequado para o RES e extratos de grainha e pele de uva. Contudo, a otimização destas nanopartículas deve ser realizada de modo a aumentar o potencial terapêutico dos fármacos em estudo.

Palavras-chave: Doença de Alzheimer, Extrato de grainha de uva, Extrato de pele de uva, Lipossomas, Nanopartículas de PLGA, Resveratrol.

Abstract

Resveratrol (RES) has been suggested as therapeutic for Alzheimer Disease (AD). Given their many benefits of RES, it is believed that it is useful in the therapy of AD. RES has low bioavailability, resulting from its low solubility in water and rapid clearance from the circulation of RES make difficult to establish bio efficacious concentrations of RES in the blood and tissues of humans. Therefore, new therapeutic strategies, as specific drug delivery systems, must be developed in order to overcome those limitations. In this work, RES and grape seed and skin extracts were encapsulated in liposomes and poly(lactide-co-glycolide) nanoparticles (PLGA NPs). Liposomes and PLGA NPs with controlled sizes and properties were prepared using the hydration of a thin lipid film method and the single emulsion solvent evaporation methods, respectively. No significant values of encapsulation efficiency were obtained for liposomes The prepared PLGA NPs exhibit a spherical shape, mean diameter between 158 to 182 nm, low PdI values and negative zeta potential values. While RES entrapment reached values of efficiency of approximately 80±6 %, for grape seed and skin extracts-loaded PLGA NPs the attained encapsulation efficiency values were slightly lower, 75±5 % and 74±8 %, respectively. The prepared system is stable at storage conditions for one month. ThT binding assay and TEM results demonstrated that the drugs used inhibit the $A\beta_{(1-42)}$ fibril formation. The results indicated that the extracts have a more pronounced inhibitory effect in comparison with RES. At the concentration of 40 µM, RES inhibits around 86% of the aggregation of the peptide, the grape skin extract inhibits around 92% and the grape seed extract inhibits around 97%. At the concentration of 80 µM, these values increased for 91, 97 and 98%, respectively. These results suggest that beyond to contain RES that inhibits the aggregation of $A\beta_{(1-42)}$, the extracts have other polyphenols that make this inhibitory effect most pronounced. The studies proved that drug-loaded PLGA NPs inhibit the $A\beta_{(1-42)}$ fibril formation. At the concentration of 40 µM, RES-loaded PLGA NPs inhibits around 46% of the aggregation of the peptide, the grape skin extract-loaded PLGA NPs inhibits around 52% and the grape seed extract-loaded PLGA NPs inhibits around 56%, after 10 days of incubation. From the at-

tained results, it was possible to conclude that PLGA NPs formulation is a suitable nanocarrier for RES and extracts of grape seed and skin. But, the optimization of NPs must be performed in order to increase the therapeutic potential of the drugs under study.

Keyword: Alzheimer disease, Grape seed extract, Grape skin extract, Liposomes, PLGA NPs, Resveratrol.

Acknowledgments

Contents

List of Figures

List of Tables

List of Abbreviations

A'	Photon absorption
a.a.	Amino acids
Aβ	Amyloid-beta
ABC	ATP-binding cassette
ACH	Amyloid cascade hypothesis
AD	Alzheimer's disease
ApoE	Apolopoprotein E
APP	Amyloid percursor protein
αSyn	Alpha-synuclein
ATP	Adenosine triphosphate
BBB	Blood-brain barrier
CF	Chloroform
CNS	Central nervous system
CSF	Cerebrospinal fluid
DLS	Dynamic light scattering
DMSO	Dimethyl sulfoxide
EtOH	Absolute ethanol
F	Fluorescence
HD	Huntington's disease
HCl	Hydrochloric acid
HFIP	Hexafluoro-2-propanol
HPLC	High-performance liquid chromatography
HR	Hydrodynamic radius
IC	Internal conversion
MLVs	Multilamellar vesicles
MW	Molecular weight
MWCO	Molecular weight cut-off

NaOH	Sodium hydroxide
NPs	Nanoparticles
PBS	Phosphate buffered saline
PD	Parkinson's disease
PdI	Polydispersity index
PEG	Polyethylene glycol
PGA	Poly glycolic acid
P-gp	P-glycoprotein
PLA	Poly lactic acid
PLGA	Poly (lactic-*co*-glycolic acid)
PSEN1	Presenilin 1
PSEN2	Presenilin 2
RES	Resveratrol
RNA	Ribonucleic acid
RMT	Receptor mediated transport
SDS	Sodium dodecyl sulphate
SLC	Solute carrier
SUVs	Small unilamellar vesicles
TEM	Transmission electron microscopy
ThT	Thioflavin T
Tm	Phase transition temperature
UV	Ultraviolet
WB	Western Blot

Chapter 1

Introduction

1.1 - Motivation

The incidence of Alzheimer's disease (AD), a neurodegenerative disorder, is promoted by the increase of the age. This disease affects the memory and other cognitive functions with sufficient intensity to produce a functional loss, and it is the most common cause of dementia in the elderly (Brookmeyer, et al., 2007). AD is a progressive disease and is characterized by loss of memory and cognitive impairment, loss of language and behavior changes. The neuropathological characteristics of AD include extracellular senile plaques, which consist of deposits of amyloid beta-peptide (Aß) and neurofibrillar tangles that are formed by hyperphosphorilation and abnormal deposition of tau protein (Clippingdale, et al., 2001) (Klafki, et al., 2006) (Selkoe, 2001). The imbalance between Aß production and its clearance leads to the Aß aggregation in the brain, that plays a key role in the development of AD (Li, et al., 2012).

Insoluble fibrillar protein aggregates are considered a pathological feature of several neurodegenerative diseases such as AD, PD and Huntington's disease (HD). Protein misfolding or partially folded structure is responsible for the fibrillation of various amyloidogenic proteins/peptides (Ahn, et al., 2007). Thus, it is essential to find molecules that prevent or interrupt the aggregation of proteins (Feng, et al., 2009). A key aspect to be considered is if these molecules have the ability to cross the blood-brain barrier (BBB).

Various natural compounds have been suggested as therapeutics for AD and PD. Among these compounds, resveratrol (RES) (the major phenolic constituent of red wine) arouses great interest (Amri, et al., 2012). RES has interesting biochemical and physiological properties such as antioxidant, anti-inflammatory, anticarcinogenic, analgesic, cardioprotective, chemo-preventive, anti-aging activities and neuroprotective (Ahn, et al., 2007) (Baur & Sinclair, 2006). Several studies have demonstrated that RES is capable of preventing a variety of disorders, including cardiovascular diseases, cancer, diabetes, arthritis and neurodegenerative diseases. Given the benefits of RES, it is believed that it is useful in the therapy of AD and PD (Gusman, et al., 2001). RES has anti-amyloidogenic activity because it promotes the intracellular degradation of Aß by a mechanism involving the proteasome, thereby reducing levels of Aß (Marambaud, et al., 2005).

A growing effort has being applied to find novel approaches for neurodegenerative treatment and in recent years a growing number of studies, focused on the research and development of nanoparticles as drug delivery systems, have been conducted (Wilczewska, et al., 2012). Liposomes and PLGA have different physico chemical, biochemical and mechanical properties each presenting their own advantages where drug delivery is concerned. As the success of a neurodegenerative disease therapy depends not only on the pharmacokinetic and pharmacodynamic activity of the therapeutic agent, but to a large extent, on its bioavailability and toxicity (Acharya & Sahoo, 2011), the development of a nanocarrier for RES will allow to enhance its therapeutic activity.

1.2 - Main Objectives

The main aim of the present work is to develop suitable nanoparticles (NPs) for drug delivery system for RES and extracts of seed and skin of grape. For that purpose, first, the physicochemical properties of RES and the extracts of seed and skin of grape were assessed: stability at different temperatures and pH's. Liposomes and PLGA nanoparticles with controlled sizes and properties were prepared in this study, as nanocarriers of RES and extracts of seed and skin of grape. Their synthesis was complemented with physicochemical characterization of structure and properties. The effect of RES and extracts of seed and skin of grape on Aß was studied.

1.3 – Thesis Organization

This dissertation is organized into seven chapters. This chapter, "Introduction", presents the subject and main objectives of this research work. Chapter 2, "State of the art", presents an overview of the AD, the function and importance of the BBB and drug delivery system that target Aß namely liposomes and PLGA NPs. Lastly, a review of the RES and their effects on AD and PD. Chapter 3, "Characterization of Resveratrol" the physicochemical properties of RES were assessed: stability at different temperatures and pH. Chapter 4, "Nanocarriers Preparation and Characterization", describes the methodology involved in the preparation and characterization of the liposomes and PLGA NPs. Chapter 5, "Interaction of Amyloid-Beta with Resveratrol", presents and discusses the interaction study of $A\beta_{1-42}$ with RES and extracts of seed and skin of grape. Chapter 6, "Conclusions" summarizes the main findings of this research work.

Chapter 2

State of the Art

2.1 – Alzheimer's Disease

The increase of the age promotes incidence of neurodegenerative diseases. These diseases destabilize significantly the memory and other cognitive functions with sufficient intensity to produce a functional loss, such as carrying out everyday activities or recognizing people and places (Brookmeyer, et al., 2007).

AD is known as the most important neurodegenerative disease. In 1906 was described by a German neurologist, Alois Alzheimer, and received that designation in 1910 by Kraeplin. AD is characterized by severe loss of cognitive ability, with decreased declarative memory and communication difficulties as well as psychiatric symptoms such as apathy, spatial disorientation, general disinterest and depression and agitation/aggression. The latter symptom is reflected in the early stage of the disease (Gaggelli, et al., 2006). A loss of emotional control is observed frequently in patients with AD, a symptom that is accompanied by physical or verbal aggression. With de evolution of the disease, people develop motor problems and present difficulty for walking and execute simple activities. By the time, the disease causes a progressive decline of the memory and cognition, leading to the immobility of the patients that succumb to respiratory difficulties (Larson, et al., 2004). This disease is progressive and for now irreversible. AD affects the central nervous system with psychological and physiological consequences (Blennow, et al., 2006).

AD affects individuals of any age but, normally, this disorder appears among people over the age of 65 years, with an average of eight year living after the appearance of the first symptoms (Larson, et al., 2004). Between 50-70% of people with dementia have this disease and affects about 4-10% of the population between 65 and 75 years, 10-35% between 75 and 85 years and 50% in people over 85 years (Brookmeyer, et al., 2007) (Gaggelli, et al., 2006). In real numbers, the annual incidence of dementia for AD in the United States is 350 000 cases. In European Union countries, the incidence rises to 600 000 annual cases, numbers that exceed the cerebral vascular accident, diabetes mellitus and breast cancer (Kalaria, et al., 2008). AD currently affects over 35 million people worldwide (Ferri, et al., 2005). With in-

creasing mean life expectancy, it is expected that this number will increase to 66 million by 2030 and 140 million in 2050 (Brookmeyer, et al., 2007).

The AD has two histopathological markers: neurofibrillary tangles and senile plaques (or amyloid plaques) (Clippingdale, et al., 2001) (Klafki, et al., 2006). Senile plaques consist of deposits of Aß whereas neurofibrillary tangles are formed by hyperphosphorilation and abnormal deposition of tau protein (Clippingdale, et al., 2001) (Klafki, et al., 2006) (Selkoe, 2001). The peptide is aggregated as amyloid fibrils within the neuritic plaques and vascular deposits (Selkoe, 2001). Scientific evidences from genetic and animal models have established a causative role of Aß in AD (Hardy & Selkoe, 2002).

The AD brain exhibits modified morphology, including enlargement of the ventricular system and atrophy of the frontal, temporal and parietal cortex together with the hippocampus and amygdale (Alves, et al., 2012). Initially, the senile plaques appear in the frontal cortex, and then spread throughout the cortical region. Hyperphosphorylated tau and insoluble tangles appear first in limbic system (entorhinal cortex, hippocampus, dentate gyrus), and then in the cortical region. Tangles appear before deposition of plaques being most associated with the severity of the disease than the amount of senile plaques (Hardy & Selkoe, 2002).

The AD still does not have cure, so treatment aims only to control their symptoms. The medications used include Rivastigmine, Donepezil, Galantemina and Memantine (Blennow, et al., 2006) (Kalaria, et al., 2008).

Evidence supports the existence of a direct relationship between the degree of dementia patients who have AD, and the concentration of soluble aggregates of the Aß peptide (Lee, et al., 2004). Aß is derived by proteolytic cleavage of the ß-amyloid precursor protein (APP) by sequential activities of ß- and γ-secretases. This process is explained by a theory has been formulated for 25 years: a cascade hypothesis (Clippingdale, et al., 2001) (Hardy & Selkoe, 2002) (Ladiwala, et al., 2012).

2.1.1 - Amyloid Cascade Hypothesis

The amyloid cascade hypothesis (ACH) is the most influential model of the AD pathology proposed over the last 25 years. The identification of Aß in senile plaques and genetic studies that identified mutations in the APP, presenilin 1 (PSEN1), and presenilin 2 (PSEN2) genes leading to the accumulation of Aß, resulted in the original formulation of the ACH (Reitz, 2012). As a consequence of these observations, the presence of Aß within senile plaques was interpreted as an effect of these mutations that subsequently leads to cell death and dementia (Armstrong, 2011) (Hardy & Selkoe, 2002) (Karran, et al., 2011) (Korczyn, 2008) (Reitz, 2012) (Sommer, 2002).

The amyloid cascade hypothesis (Figure 2.1) suggests that dysfunction and neuronal death in the brain is caused by the deposition of Aß. In the original hypothesis, it is proposed that this neuronal dysfunction and death was caused by the deposition of Aß fibrils in amyloid plaques. As knowledge of pathological changes in AD increased, research focused on more specific alterations in Aß processing, such as the cleavage of APP into Aß peptides ($A\beta_{1-40}$ and $A\beta_{1-42}$) and the importance of Aß oligomers (small aggregates of 2 to 12 peptides) (Armstrong, 2011) (Klafki, et al., 2006) (Sommer, 2002).

The cascade of Aß peptide aggregation involves conformational transitions of α-helices to ß-sheets. *In vitro* studies indicated that this transition conformation plays a key role in the formation of amyloid fibrils. Initially, Aß monomers are converted into soluble aggregates

designated oligomers that have a ß-sheet structure. Oligomers aggregate forming protofibrils and the aggregation of these protofibrils originates insoluble fibrils. The transition of antiparallel to parallel ß –sheet results of the conversion of oligomers into fibrils (Armstrong, 2011).
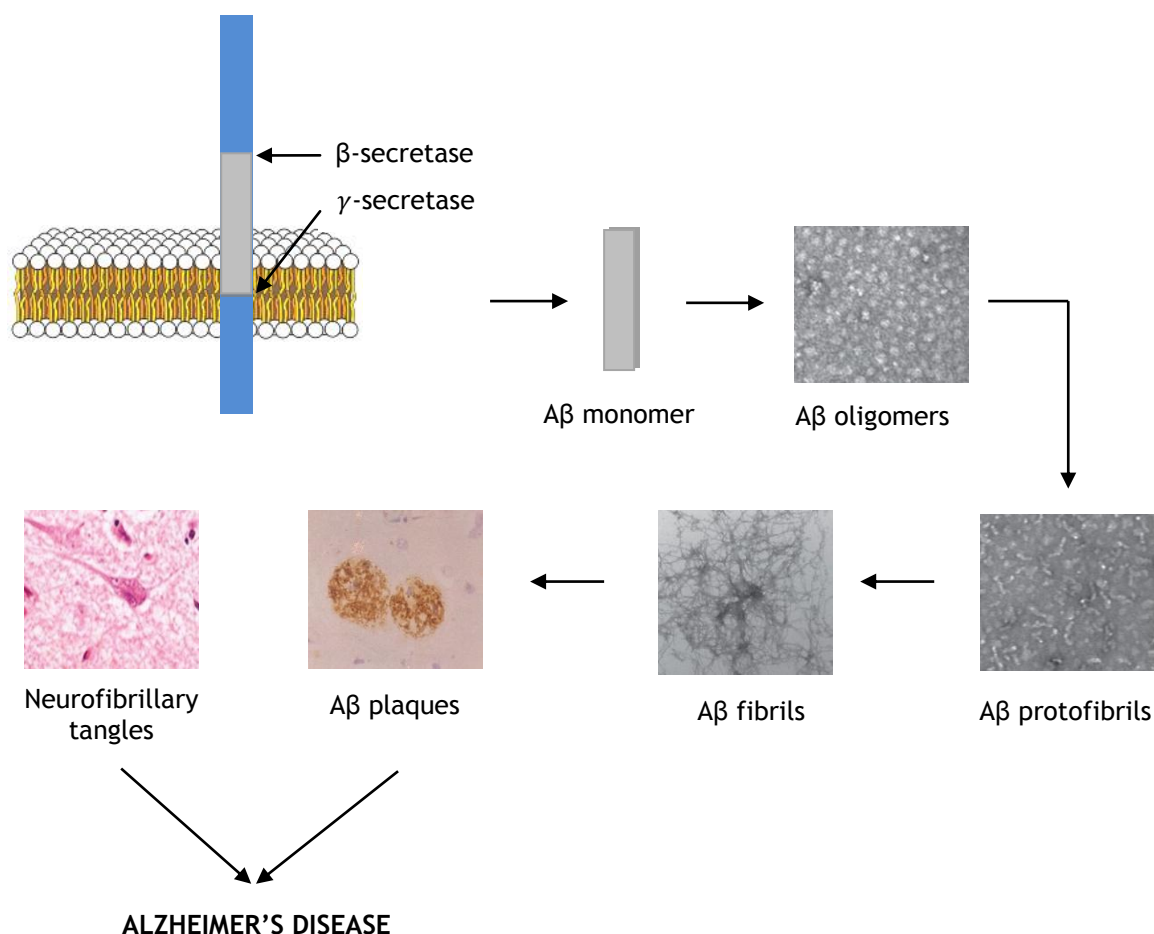
Figure 2.1 - Representation of the amyloid cascade hypothesis. Adapted from (Ahmed, et al., 2010).

Tau, a microtubule-associated protein, is the major constituent of neurofibrillary tangles. The amyloid cascade hypothesis suggests toxic concentrations of Aß cause changes in tau protein and subsequent formation of neurofibrillary tangles (Small & Duff, 2008). Tau is a soluble protein, but insoluble aggregates are produced during the formation of neurofibrillary tangles, which disrupt the structure and function of the neuron. Initially, Tau monomers bind and form oligomers, which then aggregate into a ß-sheet before form the neurofibrillary tangles (Hardy & Selkoe, 2002) (Meraz-Ríos, et al., 2010).

Aß derived from the proteolytic cleavage of APP, a protein that has the general properties of a cell surface receptor. The APP gene, located on chromosome 21, codes for multiple isoforms of a glycoprotein that contain a single membrane spanning sequence, a long N-terminal extracellular region and a short C-terminal cytoplasmic tail that is expressed in many tissues and concentrated in the synapses of neurons. This protein can be processed through two main pathways: non-amyloidogenic and amyloidogenic. In the non-amyloidogenic pathway, alpha-secretase, a proteolytic enzyme, cleaves APP in its transmembrane region

resulting in a soluble fragment of APP and a carboxy-terminal fragment C83. For the amyloidogenic pathway, the APP cleavage produces the Aß peptide through the sequential action of ß- and γ-secretase (Clippingdale, et al., 2001). After processing of APP by ß- and γ-secretase, Aß is secreted and aggregates into fibrils that deposit in senile plaques. Fibrils and plaques can induce neurotoxicity directly or indirectly, e.g. by the formation of neurofibrillary tangles (Armstrong, 2011) (Klafki, et al., 2006) (Sommer, 2002).

Originally it was thought that Aß was a product of the abnormal cleavage, but now it is known that Aß has been established as a normal metabolic product that is found in cerebrospinal fluid and serum of healthy individuals. The regulatory activity of three different proteolytic enzymes, α-, ß- and γ -secretase, in their specific cleavage sites produces various products, including $A\beta_{1-40}$ and $A\beta_{1-42}$ (Lee, et al., 2004). The most abundant forms of Aß peptide have 40 (~90%) and 42 (~10%) amino acids (a.a.). The $A\beta_{1-42}$ is characteristically produced by cleavage in the endoplasmatic reticulum, while the $A\beta_{1-40}$ normally is produced by cleavage in the trans-Golgi network. $A\beta_{1-42}$ is the main specie of Aß present in the nucleus of senile plaques although $A\beta_{1-40}$ is the predominant product of this proteolytic pathway and is found mainly in cerebrovascular amyloid deposits (Hardy & Selkoe, 2002). The deposition of $A\beta_{1-40}$ and $A\beta_{1-42}$ into senile plaques begins with the nucleation of soluble $A\beta_{1-42}$ into fibrils followed by accumulation of normally soluble $A\beta_{1-40}$ (Lee, et al., 2004). The $A\beta_{1-42}$ peptide aggregates fast than $A\beta_{1-40}$, and the ratio of these two isoforms is influenced by the pattern of cleavage - from APP by α-, ß-, and γ-secretases (Hardy & Selkoe, 2002).

Several potential risk genes for AD have been identified, with the apolipoprotein E (ApoE) considered to be the most consistent. The ApoE gene represents the major genetic risk factor for AD. Humans have three common ApoE alleles: ApoE2, ApoE3 and ApoE4. ApoE4 allele can bring forward considerably the age of disease onset, ApoE3 can be considered to be neutral and ApoE2 is thought to be protective. The apoE4 triggers the Aß fibrillogenesis by accelerating the development of AD and ApoE3 binds to tau protein (whose their function is believed to be related to stabilization of neuronal microtubules), reducing the rate of phosphorylation and the consequent development of filaments (Blennow, et al., 2006) (Gaggelli, et al., 2006). The apoE protein acts as a carrier for cholesterol brain. Cholesterol modulates the processing of APP by increasing the enzyme ß-secretase activity, resulting in increased production of Aß, leading to increasing deposits of amyloid. On the other hand, the apoE2 has a positive effect on memory and then is protective against the development of AD. The apoE4 appears to have a neurotoxic role leading to neurodegeneration and accelerates the deposition of Aß. Thus, the interaction between Aß, apoE4, cholesterol and APP forms a cascade of events that culminate in the pathogenesis of AD (Selkoe, 2001).

Individuals with two ApoE4 alleles have more than seven times increased risk of developing AD compared with those with ApoE3 alleles (Korczyn, 2008).

2.2 – Drug Delivery Systems to Cross the Blood Brain Barrier

The transport of the majority of drugs from the blood to the brain is impeded by BBB. The BBB is composed of a monolayer of brain capillary endothelial cells and its main function is to protect the brain against toxic substances (Alam, et al., 2010) (Huang, et al., 2013) (Boer & Gaillard, 2007). This BBB function results from the combination of the physical barrier, transport barrier (specific transport mechanisms mediating solute flux), and metabolic barrier

(enzymes that metabolizing molecules in transit) (Abbott, et al., 2006) (Loscher & Potschka, 2005) (Hervé, et al., 2008). Thus, the presence of the BBB difficult the development of new treatments for brain diseases (Pardridge, 2003) (Pardridge, 2012) (Pardridge, 2005). The global market of the drugs for the CNS needs to grow over 500% in order to be compared to the world market for cardiovascular drugs (Pardridge, 2002).

Nearly 100% of large-molecule drugs do not cross the BBB. Also the smaller molecules cross the BBB have difficulties in crossing the BBB. About 98% of them cannot cross this barrier (Lipinski, 2000) (Pardridge, 2003). For a small-molecule drug to cross the BBB in pharmacologically significant amounts, the molecule must have two molecular characteristics: 1) high lipid solubility and 2) low molecular mass (<400-500 Daltons) (Pardridge, 2003). Currently there are only four classes of CNS disorders that are treated with small molecule drug: depression, schizophrenia, chronic pain and epilepsy (Lipinski, 2000) (Pardridge, 2003) (Pardridge, 2005). Still, there is no neurotherapy to stop the neurodegeneration that occurs in the AD and PD (Zivadinov, et al., 2003).

Until now, several nanoparticles (NPs) have been developed to protect and transport the desired molecules to the brain (Ramos-Cabrer & Campos, 2013). NPs are nanoscaled particles (10-1000 nm), composed by natural or synthetic polymers. They interact with biological barriers crossing them easily and they are used to target and deliver drugs in a controlled manner. The NPs have proven to be the best vehicles to deliver drugs to biological systems in different neurodegenerative diseases due to their ability to cross the BBB (Liu, et al., 2012). NPs can be classified in reversible or irreversible complexes. The reversible NPs are supramolecular complexes formed by noncovalent intermolecular interactions as van de Waals forces or lipophilic interactions. Liposomes are one example of this type of nanoparticle (Ramos-Cabrer & Campos, 2013). Dendrimers, nanocapsules, nanospheres, nanocages and nanotubes are examples of non-reversible NP that comprise molecules with strong molecular interactions like covalent or metallic bonds, presenting great stability (Alam, et al., 2010) (Ramos-Cabrer & Campos, 2013).

The encapsulation of the drug into the particle is made by incorporating the molecule during the NPs production (Danhier, et al., 2012), preventing agglutination of the drug with plasmatic proteins or its retention in the liver, spleen, lungs, and others (Brigger, et al., 2002) (Kumari, et al., 2010). Sometimes is necessary to change the NPs surface for that can cross the BBB. The modifications strategies can be based on: a) covalent attachment of polyethylene glycol (PEG), b) coating with certain surfactants that should have PEG fragments in their structure and c) covalent attachment or adsorption of targeting molecules (Wohlfart, et al., 2012).

2.2.1 - Liposomes

Liposomes are vesicles formed by one or more phospholipid bilayers concentrically oriented around an aqueous compartment. This structure act as a drug carrier (Anwekar, et al., 2011) (Huang, et al., 2013) (Torchilin, 2005). These structures are formed by amphiphilic compounds that have a polar structure capable of interacting with water and a nonpolar region which tends to protect yourself from contact with water (Figure 2.2) (Shashi, et al., 2012). Liposomes allow the encapsulation of hydrophilic and/or lipophilic substances. Hydrophilic substances remain in the aqueous compartment while lipophilic substances are absorbed by the lipid membrane (Huang, et al., 2013) (Torchilin, 2005). Liposomes are spherical

lipid particles of variable size, just visible using high resolution microscopes (Malam, et al., 2009).
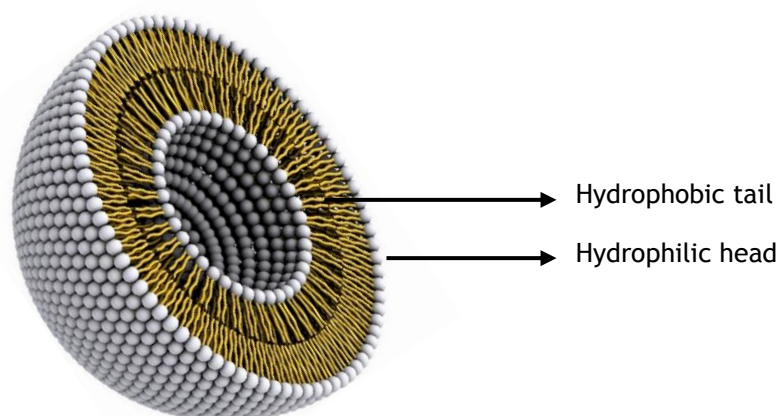
Figure 2.2 - Schematic representation of a liposome structure.

Liposomes may present different sizes, from small unilamellar vesicles (SUVs) with diameters less than 100 nm until multilamellar vesicles (MLVs) with diameters between 100 and 1000 nm. SUVs are preferred for the efficient and continuous drugs release (Liu, et al., 2012).

The controlled release systems of pharmaceuticals have been the subject of research in the last four decades. Liposomes membranes have the ability to fuse with cell membranes and then release their content into the cytoplasm. Liposomes are optimal carriers for the entrapment and cellular delivery of drugs and are able to promote a controlled release of the drugs at the target site over a prolonged period of time (Manconi, et al., 2007). Such nanocarriers are considered excellent systems for drug controlled release due to their structural flexibility, size, composition and fluidity/permeability of the lipid bilayer versatility. Another advantage is that they are able to incorporate a variety of both hydrophilic and hydrophobic compound. In general, encapsulation and retention of active substances in liposomes depend on the nature and concentration of the phospholipids, the concentration of the substance concerned and the conditions for obtaining liposomes (Mufamadi, et al., 2010).

The main advantage of the liposomes is that resemble the structure of cell membranes. Therefore, these particles effectively interact with cells and tissues. In addition, liposomes are non-toxic, biodegradable (Gonçalves, et al., 2014) (Salvati, et al., 2013) (Sirisha, et al., 2012) (Torchilin, 2005) and can be prepared synthetically at high purity (Schnyder & Huwyler, 2005).

PEG molecules are added to increase the stability and bioavailability of the systems while protecting the liposomes from clearance by cells of the reticuloendothelial system (Torchelin, et al., 1994). These drug delivery systems increase the half-life up to 90 hours in humans, due to a reduced absorption by the liver and spleen (Gabizon, et al., 2003). Cholesterol is also added to the formulations to increase the circulation time of the liposomes in the blood through the increase of their stability (Gabizon, et al., 2003) (Upadhyay, 2014).

2.2.2 – PLGA Nanoparticles

Several studies have been conducted about drug delivery by biodegradable polymers. Amongst all the biomaterials, application of the biodegradable polymer poly (lactic-*co-*

glycolic acid) (PLGA) has shown immense potential as drug delivery carrier and as scaffold for tissue engineering. PLGA is a co-polymer of poly lactic acid (PLA) and poly glycolic acid (PGA) linked by ester bonds (Figure 2.3) physically strong and highly biocompatible that has been extensively studied as delivery vehicle for drugs, proteins genes, vaccines, antigens, human growth factors and various other macromolecules such as DNA, RNA and peptides (Acharya & Sahoo, 2011) (Makadia & Siegel, 2011). PLGA is most popular among the various available bio-degradable polymers due to their nontoxic behavior, stability in blood, nonthrombogenic, nonimmunogenic, noninflammatory, do not activate neutrophils, excellent biocompatibility, and biodegradability properties, long clinical experience, favorable degradation characteristics, possibilities for sustained drug delivery and its hydrolysis leads to metabolite monomers, lactic acid and glycolic acid (Figure 2.4) (Acharya & Sahoo, 2011) (Kumari, et al., 2010) (Makadia & Siegel, 2011). Because these two monomers are endogenous and easily metabolized by the body via the Krebs cycle, a minimal systemic toxicity is associated with the use of PLGA for drug delivery or biomaterial applications (Acharya & Sahoo, 2011) (Kumari, et al., 2010).
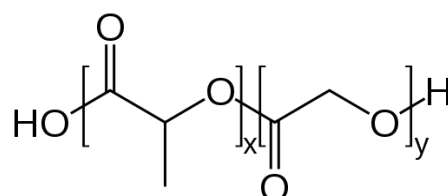
Figure 2.3 - Chemical structure of poly (lactic-co-glycolic acid). x represents the number of lactic acid units and y is the number of glycolic acid units.

PLGA is soluble in wide range of common solvents including chlorinated solvents, tetrahydofuran, acetone or ethyl acetate. In water, PLGA biodegrades by hydrolysis of its ester linkages (Figure 2.4). During hydrolysis the increasing number of free carboxylic end-groups lead to matrix swelling and increasing of hydrophilicity, which enhances water-uptake (Wischke & Schwendeman, 2008). These acidic products accumulate inside the PLGA NPs and are responsible for reaction auto-catalysis (Klose, et al., 2008) (Wischke & Schwendeman, 2008). The hydrolytic breakdown also causes the formation of pores in the matrix of the polymeric system (Cohen, et al., 1991). The change in PLGA properties during polymer biodegradation influences the release and degradation rates of incorporated drug molecules (Makadia & Siegel, 2011).

PLGA   Lactic acid   Glycolic acid
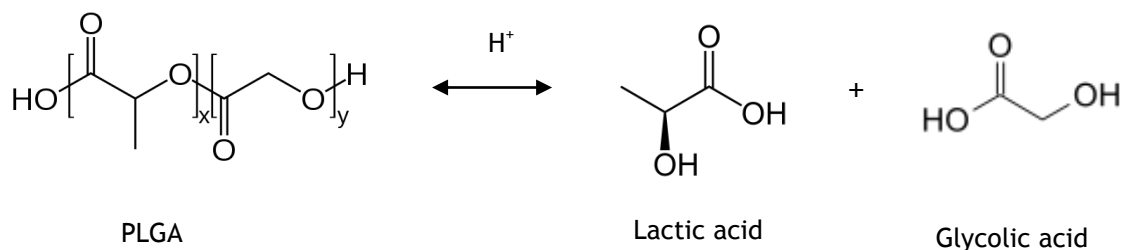
Figure 2.4 - Representation of hydrolytic degradation of PLGA and its products. Adapted from (Danhier, et al., 2012).

Although not causing tissue damages, PLGA NPs are not able to remain for a long time in blood stream because they are usually recognized by the immune system. Though, the size of the PLGA NPs influences the blood circulation time (Acharya & Sahoo, 2011). If the system is smaller than 100 nm, the plasma protein adsorption to the NP surface is almost negligible, and the immune system is unable to eliminate NPs. For NPs over 100 nm, their surface must be functionalized with biomolecules to increase blood circulation half-life. One of the most used strategies is coating their surface with a biodegradable copolymer with hydrophilic characteristics such as polyethylene glycol (PEG) (Wang, et al., 2009).

Several studies have investigated the mechanism of intracellular drug delivery by PLGA NPs. PLGA NPs are internalized in cells partly through fluid phase pinocytosis and also through receptor-mediated endocytosis. The acidic medium of late endosome triggers a charge change in PLGA NPs. The NP becomes cationic leading to destabilization of late-endosomal membrane allowing efflux of NP and drug release (Figure 2.5). PLGA NPs rapidly escape the endosome-lysosomes and enter the cytoplasm. This facilitates interactions of NPs with the vesicular membranes leading to transient and localized destabilization of the membrane resulting in the escape of NPs into the cytosol (Acharya & Sahoo, 2011) (Vasir & Labhasetwar, 2007). Endosome-lysosome pathway is characterized by two types of compartments, the endosome and lysosome. Lysosomes are usually regarded as the terminal degradation compartment of this pathway. One important feature of PLGA NPs is that they are cationic only in the endosomal compartment and do not destabilize the lysosomes, unlike another kinds of NPs. This allows reducing their toxicity (Acharya & Sahoo, 2011).
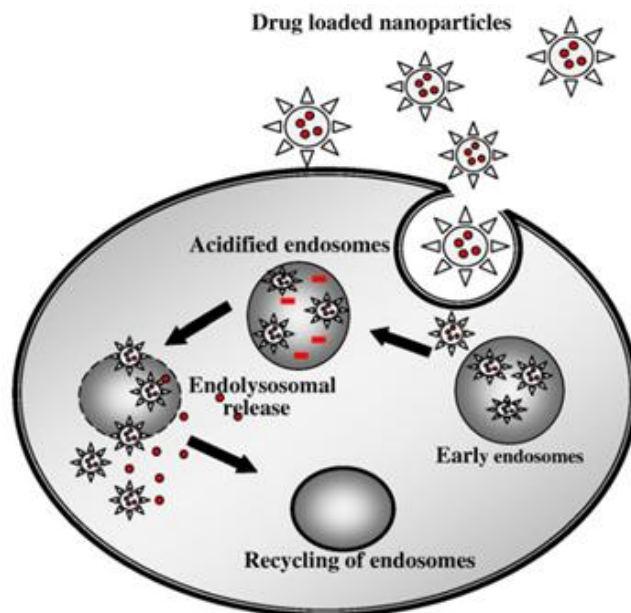
Figure 2.5 - PLGA NPs endolysosomal efflux and drug release. Adapted from (Danhier, et al., 2012).

Several factors affect the PLGA NPs release profile such as: 1) drug's chemical structure and its interactions with PLGA; 2) physico-chemical properties of the encapsulated drug; 3) geometry of drug-loaded PLGA NPs (size and shape); 4) drug solubility and 5) loading efficiency (Cohen, et al., 1991) (Kumari, et al., 2010) (Wang, et al., 2009). The main pathways for

drug release in PLGA NPs are: 1) desorption of drug bound to the surface, 2) diffusion through NP matrix, 3) NP matrix hydrolysis, 4) or a combined degradation-diffusion process (Cohen, et al., 1991) (Klose, et al., 2008) (Kumari, et al., 2010) (Makadia & Siegel, 2011). PLGA NPs generally exhibit a biphasic release profile, characterized by an initial burst due to the release of surface-adsorbed drugs followed by a biodegradation-accelerated release until complete polymer solubilization (Kawasaki & Player, 2005) (Kumari, et al., 2010). This final phase is a combination of biodegradation-diffusion process. This final phase is a combination of biodegradation-diffusion process (Kawasaki & Player, 2005). This controlled and sustained release prevents high doses of drug accumulation. Also, the slow release allows a decrease of the administration frequency, since drug levels are maintained over long periods of time (Kumari, et al., 2010).

Despite of being widely used in medical applications, the PLGA NPs use faces a few limitations as their poor loading capacity. The burst release mentioned above can be a big disadvantage since large amounts of drug are lost before reaching the target tissue, resulting in an efficacy loss of the delivery of drugs. Also, the many required steps for NPs production such as centrifugation and dialysis are expensive and difficult to scale-up (Danhier, et al., 2012). PLGA NPs also exhibit a size-dependent cytotoxicity. Small PLGA NPs may trigger the generation of reactive oxygen species, mitochondrial depolarization and inflammatory cytokines release. Therefore, some studies indicate that PLGA NPs larger than 100 nm are safer for biomedical applications (Xiong, et al., 2013). Another drawback of these NPs is the entrapment of hydrophilic drugs, since those drugs rapidly partition into the aqueous phase during NPs preparation. Therefore is necessary to use appropriate preparation methods as the double emulsion technique (Makadia & Siegel, 2011). Finally, it is essential to functionalize the NP surface in order to achieve a maximum efficacy (Wang, et al., 2009).

2.3 – Resveratrol

RES ($C_{14}H_{12}O_3$), chemically known as 3, 5, 4' - trihydroxystilbene is a natural non-flavonoid polyphenolic compound present in over than 70 species of plants including vegetables, fruits, grains, roots, flowers, seeds, tea and wine (Amri, et al., 2012) (Chachay, et al., 2011). As more intense the color, higher is the amount of polyphenols (Li, et al., 2012). Chemically, RES has two geometrical isomers (Figure 2.6), *trans*-RES and *cis*-RES, with the *trans* form as the biologically active form (Filip, et al., 2013). RES is a highly photosensitive compound susceptible to UV-induced isomerization, since more than 80% of the *trans*-RES in solution is converted to *cis*-RES if exposed to light for 1h (Vian, et al., 2005).

Trans-RES has effects on many metabolic processes and has been suggested to modulate cardiovascular disease, inflammation, cancer, obesity, diabetes, and neurodegenerative diseases (Giovinazzo, et al., 2012) (Patel, et al., 2011). Some authors have affirmed that RES displays wide pharmacological activities such as antioxidant, anti-inflammatory, anticarcinogenic, analgesic, cardioprotective, chemo-preventive, anti-aging activities and neuroprotective (Baur & Sinclair, 2006) in some neurological disorders, such as AD, PD, HD, brain ischemia and epilepsy (Gusman, et al., 2001). Many studies confirm that RES acts in CNS. RES can pass through the BBB (Baur & Sinclair, 2006) and induce protective effects in neurodegenerative diseases such as cerebral ischemia (Gao, et al., 2006), AD (Marambaud, et al., 2005) and PD (Okawara, et al., 2007).
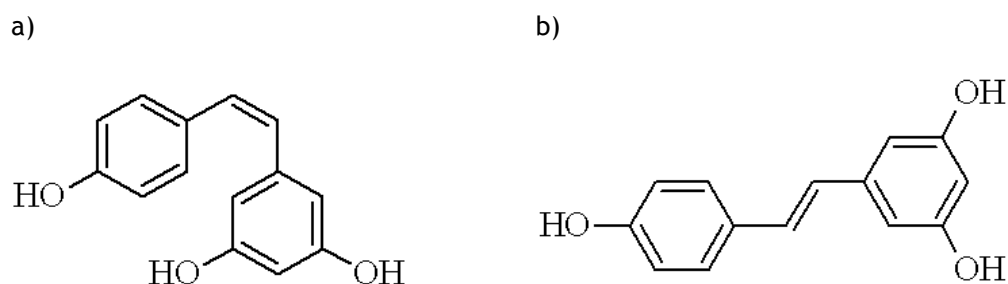
Figure 2.6 - Chemical structures of resveratrol isomers. a) *cis*-RES, and b) *trans*-RES.

RES has low bioavailability, resulting from its low solubility in water (less than 0,05 mg/ml) (Amri, et al., 2012) (Walle, 2011). The low bioavailability and rapid clearance from the circulation of RES make difficult to establish bio efficacious concentrations of RES in the blood and tissues of humans. RES can be dissolved in various common organic solvents, such as ether, ethanol, methanol, dimethyl sulfoxide (DMSO), but hardly dissolved in water (Walle, 2011).

RES has several disadvantageous properties that justify its encapsulation in carriers, such as: poor water solubility, short biological half-life, chemical instability and its rapid metabolism and elimination (Nicolás, et al., 2006).

Through the encapsulation is possible to increase the RES solubility in water and thereby also improve its bioavailability. Encapsulation may be used to stabilize RES against degradation (Amri, et al., 2012). The carrier aims to increase the therapeutic potential of RES, preventing their degradation and simultaneously cause side effects elsewhere in the body (Kristl, et al., 2009) (Mufamadi, et al., 2010).

2.3.1 – Effect of Resveratrol on Alzheimer's Disease

Several data support the role of oxidative stress in neurodegenerative diseases including AD and consequently support the beneficial effect of antioxidant as therapy of these diseases (Li, et al., 2006) (Robb, et al., 2008) (Sun, et al., 2010). Oxidative stress induces neuronal damages and modulates intracellular signaling, leading to neuronal death by apoptosis or necrosis (Li, et al., 2012). Various clinical studies indicate that antioxidants may delay the appearance of neurodegenerative diseases (Engelhart, et al., 2002) (Morris, et al., 2002). Natural compounds such as RES and other herbs have a variety of functions becoming candidates for a new generation of drugs for the treatment of patients with AD (Anekonda & Reddy, 2005) (Howes & Houghton, 2003).

In vitro studies suggest that RES may protect against oxidative damage induced by Aβ (Conte, et al., 2003) (Jang & Surh, 2003) (Kim, et al., 2007), and may encourage Aβ clearance through promotion of intracellular proteosomal activity (Marambaud, et al., 2005) (Saiko, et al., 2008).

Human sirtuins are coded by seven different genes (SIRT1 to SIRT7), whose their functions are still being investigated (Haigis & Guarente, 2006) (Michan & Sinclair, 2007). Sirtuins are located in different tissue types and they are classified into four classes of proteins: SIRT1–3 (class I), SIRT4 (class II), SIRT5 (class III), and SIRT6–7 (class IV) (Frye, 2000) (Shi, et al., 2005). SIRT1, SIRT6, and SIRT7 are localized in nucleus, with SIRT6 localized specifically in heterochromatic regions and SIRT7 in nucleoli (Michishita, et al., 2005). SIRT2 is localized in cyto-

plasm, and SIRT3, SIRT4, and SIRT5, in mitochondria (Frye, 2000) (Michishita, et al., 2005) (Shi, et al., 2005). SIRT1 appears to have a role in the basic processes related to mammal senescence such as food and glucose metabolism, adipose tissue homeostasis or DNA repair (Rodgers & Puigserver, 2007) (Qiang, et al., 2007) (Wang, et al., 2006). RES has been intensively investigated as an enzyme activator of SIRT1 (Chen, et al., 2005) (Kim, et al., 2007) (Parker, et al., 2005) (Qin, et al., 2006). RES is capable of binding to the N-terminal of SIRT1 increasing their activity (Milne & Denu, 2008). In the model of AD, the direct introduction of RES in the cerebral ventricles reduces neuronal death in the hippocampus, avoids learning difficulties and reduces the acetylation of the known SIRT1 substrates PGC-1 α and p53 (Anekonda, 2006) (Karuppagounder, et al., 2009) (Kim, et al., 2007). SIRT1 activation or overexpression was reported as neuroprotective in models of AD, by a still unknown mechanism (Chen, et al., 2005) (Kim, et al., 2007) (Parker, et al., 2005) (Qin, et al., 2006).

Studies suggest that RES can prevent $A\beta_{42}$ toxicity by direct interaction with $A\beta_{42}$ fibrils due to the fact that RES destabilizes the $A\beta_{42}$ fibrils and delays oligomers and fibrils formation of $A\beta_{42}$ (Ahn, et al., 2007) (Albani, et al., 2009) (Feng, et al., 2009) (Jang, et al., 2007) (Rivière, et al., 2007). This property of reducing the $A\beta$ toxicity seems to be a general feature of polyphenols (Albani, et al., 2010) (Feng, et al., 2009) (Ono, et al., 2008). In addition, RES reduces the $A\beta$ levels by promoting a non-amyloidogenic processing of APP and promoting clearance of intracellular $A\beta$ via the proteasomes (Li, et al., 2012) (Marambaud, et al., 2005). There is clear evidence that a decrease in proteasome activity occurs in AD brains (Keller, et al., 2000) (Salon, et al., 2000). Studies propose that $A\beta$ can lead to inhibition of proteasome, suggesting that high levels of $A\beta$ in AD brain can create a vicious cycle by inhibiting the proteasome and blocking the degradation of critical regulators of its own clearance (Marambaud, et al., 2005) (Saiko, et al., 2008).

Chapter 3

Characterization of Resveratrol

Trans-resveratrol (RES) is a natural nonflavonoid poly-phenolic compound present in over than 70 species of plants including vegetables, fruits, grains, roots, flowers, seeds, tea and wine (Amri, et al., 2012) (Chachay, et al., 2011). Chemically, RES has two geometrical isomers (Figure 2.9), *trans*-RES and *cis*-RES, with the *trans* form as the biologically active form (Filip, et al., 2013). RES is a highly photosensitive compound susceptible to UV-induced isomerization, since more than 80% of the *trans*-RES in solution is converted to *cis*-RES if exposed to light for 1h (Vian, et al., 2005).

RES has interesting biochemical and physiological properties such as antioxidant, anti-inflammatory, anticarcinogenic, analgesic, cardioprotective, chemo-preventive, anti-aging activities and neuroprotective (Ahn, et al., 2007) (Baur & Sinclair, 2006) (Gusman, et al., 2001). Many studies confirm that RES acts in CNS. RES can pass through the BBB (Baur & Sinclair, 2006) and induce protective effects in neurodegenerative diseases such as cerebral ischemia (Gao, et al., 2006), AD (Marambaud, et al., 2005) and PD (Okawara, et al., 2007). RES has anti-amyloidogenic activity because it promotes the intracellular degradation of Aß by a mechanism involving the proteasome, thereby reducing levels of Aß (Marambaud, et al., 2005).

RES has several disadvantageous properties that justify its encapsulation in carriers, such as: poor water solubility, short biological half-life, chemical instability and its rapid metabolism and elimination (Nicolás, et al., 2006). Through the encapsulation is possible to increase the RES solubility in water and thereby also improve its bioavailability. Encapsulation may be used to stabilize RES against degradation (Amri, et al., 2012) and increase the therapeutic potential of RES (Kristl, et al., 2009) (Mufamadi, et al., 2010).

3.1 – Material and Methods

3.1.1 –Resveratrol's Solutions

Trans-resveratrol ($C_{14}H_{12}O_3$ or 3, 5, 4'-trihydroxystilbene, purity ≥ 99%, molecular weight (MW) 228.24) was purchased from Sigma-Aldrich (St. Louis, MO, USA). Extracts of the grape seed and grape skin (purity ≥ 95%) was purchased from Monteloeder (Elche, Alicante, Spain). Stock solutions were prepared by dissolving RES, grape seed extract and grape skin extract in phosphate buffered saline (PBS), pH 7.4 (PBS, 10 mM phosphate buffer, 2.7 mM potassium chloride and 137 mM sodium chloride, Sigma-Aldrich). The buffer was prepared previously with ultrapure water purified with Mili-Q equipment with the specific resistance of 18.2 MΩ·cm (Milli-Q Academic, Millipore, France). To ensure complete dissolution, the three solutions were placed in the bath at 70°C for 10 minutes (Thermo Scientific Haake DC10-P5/U Heating Circulator Baths, Termo Fisher Scientific, USA). Solutions of the extracts of the grape seed and grape skin were exposed to centrifugal force under 14 000 rpm for 15 minutes (MiniSpin plus, eppendorf, Germany) and the supernatant used.

To produce a linear calibration curve of RES dissolved in PBS, solutions were prepared at 0, 5, 10, 15, 20, 25, 30, 35, 40, 50, 60, 70 and 80 µM. The absorbance of the samples at wavelength 305 nm was measured using BioTek® Synergy 2 Multi-Mode Reader (Winooski, Vermont, USA) and UV-1700 PharmaSpec UV-VIS Spectrophotometer Shimadzu (Kyoto, Japan).

3.1.2 –Ultraviolet Spectrophotometry

Radiation spectrophotometry in the ultraviolet (UV) region is widely used for qualitative or quantitative analysis due to its accuracy and, therefore, useful in several areas such as chemistry, physics, biochemistry, engineering materials, among others (Rocha & Teixeira, 2004).

The spectrophotometry is a method to measure the amount of light that absorbs a chemical substance through measurement of light intensity of a light beam that passes through a given solution. When a solution with absorbent molecules is crossed by a beam of monochromatic light of this light is absorbed by the solution and the rest is transmitted. Light absorption is also influenced by the concentration of the absorbing molecules (El-Kabbany, et al., 2014).

It can also be used to measure the concentration of a chemical known in an easy, practical and fast way. Therefore, spectrophotometry studies the interaction of electromagnetic radiation with matter (El-Kabbany, et al., 2014) (Rocha & Teixeira, 2004).

The instrument used in UV spectrophotometry is the spectrophotometer. A transparent cell which does not absorb radiation in the wavelength range used (the wavelength range of UV radiation is considered to be between 200 and 400 nm), commonly called *cuvette* is filled with the liquid sample and placed in the spectrophotometer. To get information about the absorbance of a sample it is inserted in the optical path of the apparatus where UV light passes through the sample which enables the spectrophotometer to measure the amount of light that is absorbed (El-Kabbany, et al., 2014) (Rocha & Teixeira, 2004).

The interaction of UV radiation with matter can provides information about substances by the analysis of the UV spectrum. This spectrum is a graphical representation of the relationship of the absorption of the radiation, by the substance in study, as a function of the radia-

tion wavelength. The analysis of this spectrum allows concluding the range of wavelength that the substance has a greater tendency to absorb UV radiation (Rocha & Teixeira, 2004).

A common spectrophotometer has in its constitution a radiation source and a detector. The radiation source focuses a light beam which travels through a path reaching the sample. In the sample part of the radiation is absorbed, and only some of it transmitted through the sample reaching the detector. Thus, the amount of absorbed radiation is determined by the difference between the incident light (I_0) and the light which effectively reaches the detector (I) (Figure 3.1). This relationship is translated by the equation 3.1 (El-Kabbany, et al., 2014):

$$A = -log_{10}\left(\frac{I}{I_0}\right) , \qquad (3.1)$$

where A is the absorbance; I, the light that was through the sample and reached the detector; and I_0, the incident light.
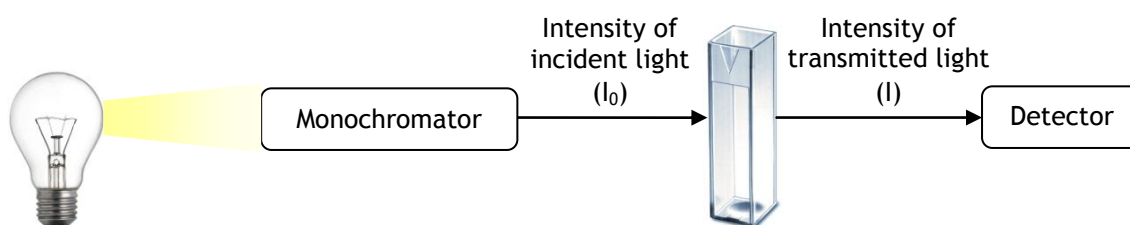
Figure 3.1 - Schematic representation of the basic principle of UV spectrophotometry.

Quantification of substances by spectrophotometry is based on the Lambert-Beer law (Equation 3.2). This law is the mathematical basis for the measurement of radiation absorption by the sample in UV regions of the electromagnetic spectrum.

$$A = \varepsilon.c.l , \qquad (3.2)$$

where A is the absorbance; ε, the molar absorptivity; c, the sample concentration; and l, the path length (El-Kabbany, et al., 2014).

Some aspects have to be taken in consideration, in order to obtain a consolidated analysis. The solute must be dissolved in a solvent and the solvent must be transparent over the wavelength range of interest. Therefore, the choice of the solvent must be done carefully since it may affect the appearance of the spectrum as they can shift the position of the absorption band. Also, if the solute isn't dissolved completely, undissolved particles can scatter light from the light source. Particles aggregates may also distort the results since as the distance between molecules become smaller the charge distribution will be affected which alter the molecules ability to absorb a specific wavelength. All this can result in errors in the analyses (Rocha & Teixeira, 2004).

3.2 – Results and Discussion

3.2.1 – Calibration Curve

To produce a linear calibration curve of RES dissolved in PBS, solutions with concentrations known were prepared and the absorbance of the samples at wavelength 305 nm was measured using BioTek® Synergy 2 Multi-Mode Reader (Winooski, Vermont, USA) and UV-1700 PharmaSpec UV-VIS Spectrophotometer Shimadzu (Kyoto, Japan) and two calibration curves were obtained (Appendix 1 and Appendix 2, respectively).

The results of calibration curves demonstrate that the calibration curves obtained have excellent linear relationship between concentration and absorbance, which translates into a coefficient of determination (R^2) of 0.995. It can be concluded also that the calibration curves have different sensitivities, result of the different sensitivities of the equipment used.

3.2.2 – Resveratrol's percentage in extracts

The percentage of RES presented in the two extracts were determined in three solutions were prepared in PBS, one solution containing RES, another with grape seed extract, and another grape skin extract, all at a concentration of 18.26 µg/ml. The absorbencies of the samples were read at a wavelength of 305 nm using BioTek® Synergy 2 Multi-Mode reader (Winooski, Vermont, USA) and were converted to concentrations through the RES calibration curve. Determined the concentrations of the samples, the percentages of RES contained in the two extracts were calculated. The concentrations obtained were 4.72% and 3.81% of the RES in the seed extract and in the grape skin extract, respectively.

Iacopini, et al. used HPLC–UV to quantify the amount of RES in seed and skin of the grape. The authors studied the total RES content in ten grape varieties. In all varieties, only a very small concentration of RES was detected, ranging between 0.670 ± 0.16 and 25.57 ± 1.16 mg/100g of seeds and skins extracts, depending of the grape varieties (Iacopini, et al., 2008). This values account for about 0.00067 and 0.02557% of RES present in extracts. Sun et al. quantified the amount of RES by HPLC in seed and skin of the grape and reported that the levels of RES were extremely low, around 6.8 mg/kg (Sun, et al., 2006) which is equivalent to approximately 0.00068%.

The difference between the published literature and this work were significantly different. These differences can be explained by the fact that the large amount of different flavonoids is present in skin and seeds grape. Given that the absorbance of flavonoids is maximum in the region of 304-350 nm (Santos, et al., s.d.), the absorbance obtained at a wavelength of 305 nm may not be due only to the RES.

3.2.3 – Stability Studies

The stability of RES and seed and skin grape extracts was analyzed at different temperatures and pHs.

3.2.3.1 – Stability Study with Temperature

To study the stability of the RES and the extracts, depending on the temperature, solutions were prepared in PBS at a concentration of 80 µM and stored at 4 °C, 25 °C (room tem-

perature) and 37 °C (physiological body temperature) for a period of two weeks. Every days, the UV-spectrum of the samples was measured. Regardless of the storage temperature of the samples it was found that the maximum absorbance of RES always occurs at a wavelength of 305 nm.

The results of stability studies with temperature (Figure 3.2 a) demonstrated that RES is stable when stored at 4 °C. The absorbance at 4 ℃ doesn't show statistically significant differences ($P<0.050$) along the days. At 23 and 37 °C, the absorbance of RES at 305 nm decreases around 44% and 63%, in 7th day and 60% and 76%, in 14th day, respectively, which suggests that the temperature increase promotes the degradation of the RES. Thus, the degradation process of RES exhibits sensitivity to temperature. Therefore, at 37 °C degradation was fast, whereas the storage at 4 °C slowed the reaction by the decreased molecular mobility. Relative to the extracts the results demonstrated that the absorbance of the samples at 305 nm doesn't show the statistically significant differences ($P<0.050$) along the days independently of temperature used in the solution store (Figure 3.2 b) and c)). This suggests that the extracts are stable for a period of 14 days at 4, 23 and 37 °C.

The impact of temperature on RES stability was studied at different temperatures is referred in literature. Zupančič, et al. prepared solutions of RES in buffers with pH 7.4 and stored at −22, 4, 25, and 37 °C for three months. The authors demonstrated that at pH 7.4 RES rapidly degraded at 25 and 37 °C, whereas the degradation was slowed at 4 °C and prevented at −22 °C (Zupančič, et al., 2015). Thus, RES stability can be increased with lower temperatures, as our findings confirmed. Liazid, et al. showed that when RES was exposed for 20 minutes to increased temperatures the extent of degradation is 17% at 125 ℃, 39% at 150 ℃, and 70% at 175 °C (Liazid, et al., 2007).

3.2.3.2 – Stability Study with pH

To study the stability of RES and extracts depending on the pH, RES solutions were prepared in PBS at a concentration of 80 μM and extract solutions at a concentration of 85 μg/ml. Five different pH values were used: 4, 5, 7.4, 8 and 11. The samples were stored at 4 °C and the UV-spectrums were measured in the wavelength range of 200 to 400 nm, for a period of 7 days.

The results of stability studies with pH (Figure 3.3) demonstrated that RES (Figure 3.3 a)) is stable at pH values below 7.4. At pH 8, the absorbance values slightly decreased but the peak of maximum absorption remains at 305 nm. At pH 10, the absorbance of RES decreased significantly and the peak of maximum absorption changed to 318 nm. Thus, these results suggest that RES is stable only for acidic pHs and neutral pH whereas basic pHs promote their degradation. Relative to the Figure 3.3 b) and c), the results demonstrated that the extracts aren't stable only for pH 10. In this case the peak of maximum absorption suffered a detour and the absorbance of extracts increased lightly. Over the 7 days, at pH acid, UV-spectrum of the RES and extract didn't change while with basic pH was found to degradation of the RES and extracts even when stored at 4 °C.

The effect of pH on RES stability has been investigated in a study of Trela & Waterhouse showing that RES is stable in buffers with pH 1, 3.5, and 7.0 for 28 days, whereas at pH 10 it rapidly degraded with a half-life of only 1.6 hours (Trela & Waterhouse, 1996). Zupančič, et al. prepared solutions of RES in buffers with pH 1.2, 6.8, 7.4, 8, 9 and 10 and stored at 4 °C for three months. RES was relatively stable in acidic conditions, whereas its degradation rate

exponentially increases in alkaline ones. The authors suggest that RES was stable in acidic pH because its hydroxyl groups were protected from radical oxidation by positively charged H_3O^+ (Zupančič, et al., 2015).
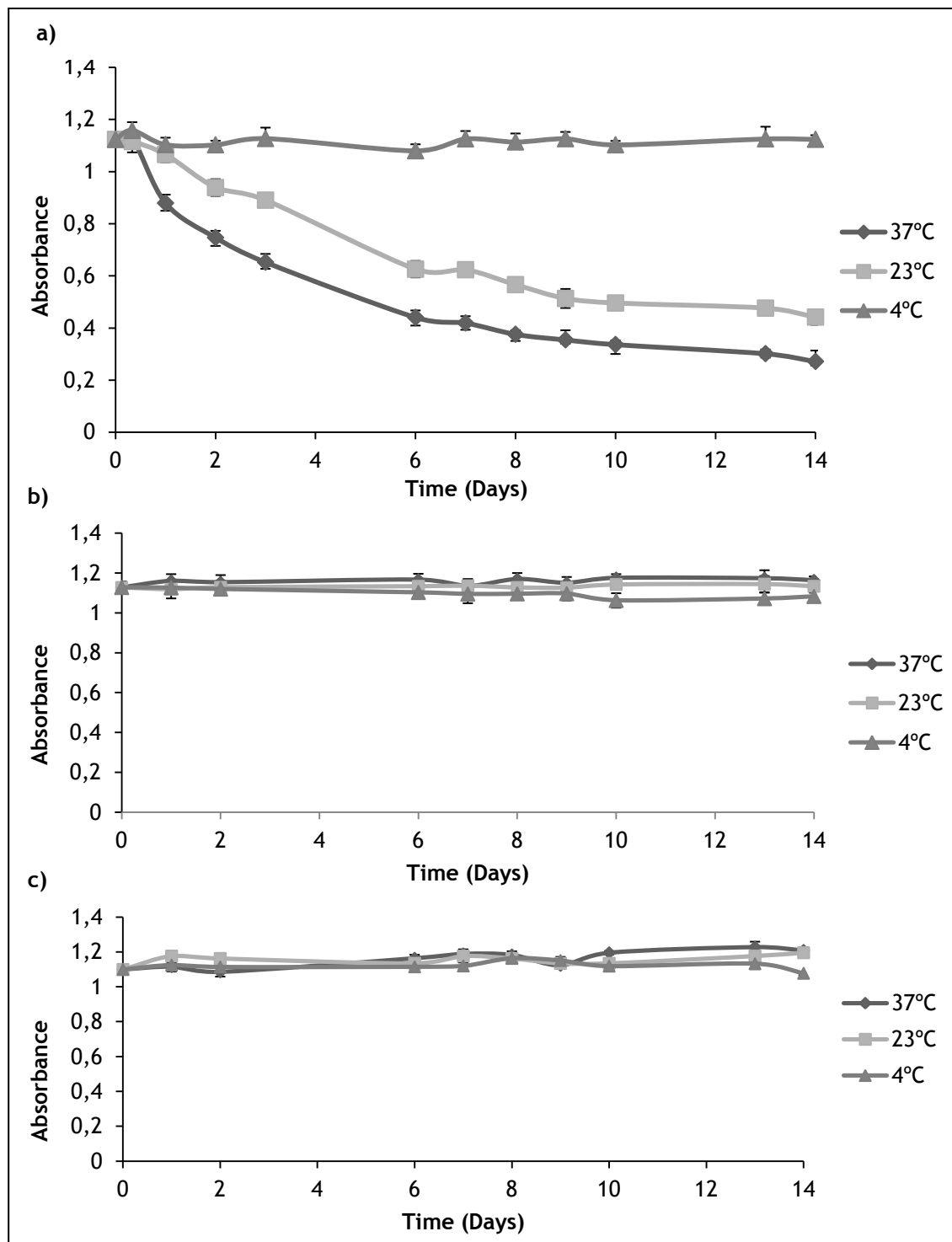
Figure 3.2 – Absorbance at a wavelength of 305 nm of **a)** RES, **b)** skin grape extract and **c)** seed grape extract. The samples were stored at 37°C, 23°C and 4°C for 14 days (n=3).
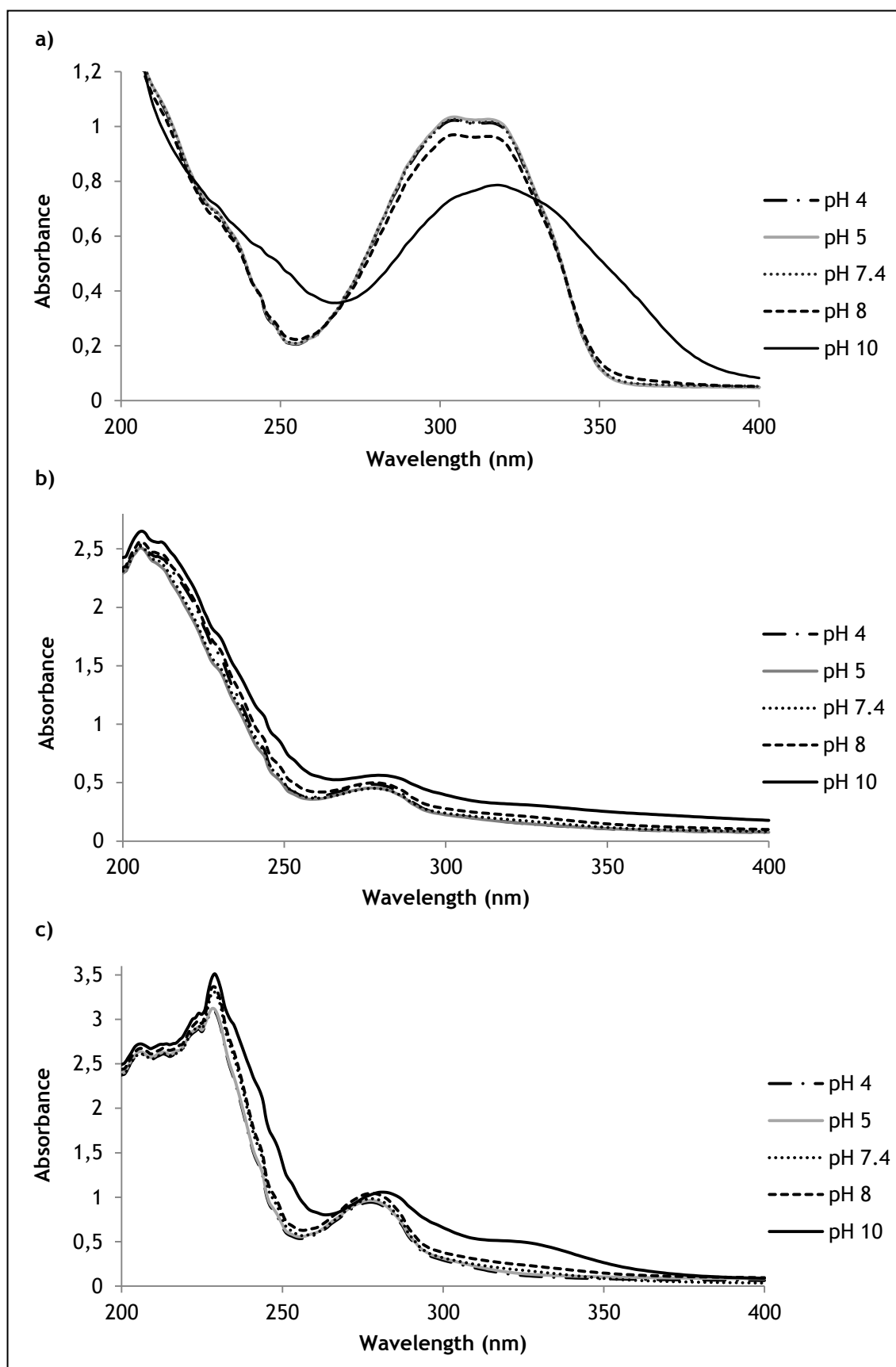
Figure 3.3 – UV-spectrum of **a)** RES, **b)** grape skin extract and **c)** grape seed extract, at pH values of 4, 5, 7.4, 8 and 10. These results are relative to the first day.

Chapter 4

Nanocarriers Preparation and Characterization

Many advantages of NP-based drug delivery have been recognized. The NPs improves the bio-availability by enhancing aqueous solubility, increases resistance time in the body (increasing half life of drug systemic circulation for clearance), releases drugs at a sustained rate and thus lowers the frequency of administration and target the drug to specific location in the body (its site of action) (Mudshinge, et al., 2011) (Zhang, et al., 2008).

A growing effort has being applied to find novel approaches for neurodegenerative treatment and in recent years a growing number of studies, focused on the research and development of nanoparticles as drug delivery systems, have been conducted (Wilczewska, et al., 2012). Liposomes and PLGA have different physico chemical, biochemical and mechanical properties each presenting their own advantages where drug delivery is concerned. As the success of a neurodegenerative disease therapy depends not only on the pharmacokinetic and pharmacodynamic activity of the therapeutic agent, but to a large extent, on its bioavailability and toxicity (Acharya & Sahoo, 2011), the development of a nanocarrier for RES will allow to enhance its therapeutic activity.

4.1 – Material and Methods

4.1.1 – Liposomes Preparation

Hydration of a thin lipid film is the original method initially used for liposomes production (Laouini, et al., 2012). This method continue to be the most common and simple method for preparation of MLVs (Popovska, et al., 2013) (Sirisha, et al., 2012). The lipids must first be dissolved and mixed in an organic solvent to assure a homogeneous mixture of lipids. Usually this process is carried out using chloroform (CF), dichloromethane, ethanol or a mixture of chloroform and methanol. Then, the organic solvent was removed by evaporation to yield a

lipid film. For small volumes of organic solvent, the solvent may be evaporated using dry nitrogen in a fume hood. For larger volumes, the organic solvent should be removed by rotary evaporation yielding a thin lipid film on the sides of a round bottom flask. To remove residual organic solvent the thin lipid film is placed on a vacuum pump overnight (Dua, et al., 2012). Finally, the dry lipidic film deposited on the flask wall is hydrated by adding an aqueous buffer solution under agitation at temperature above the phase transition temperature of lipid (Tm) (Laouini, et al., 2012) (Popovska, et al., 2013) (Sirisha, et al., 2012). When hydrated, phospholipids spontaneously assemble into liposomes due to their amphiphilic nature. They tend to assemble in vesicles in order to decrease the system free energy, by decreasing the water contact of phospholipids hydrophobic tails (Dua, et al., 2012). Depending upon their solubilities the compounds to be encapsulated can be added either to aqueous buffer or to organic solvent containing lipids (Sirisha, et al., 2012). The dispersed phospholipids in aqueous buffer yield a population of MLVs heterogeneous both in size and shape. Thus, liposome size reduction techniques, such as sonication for SUVs formation or extrusion through polycarbonate filters forming SUVs are useful to produce a population with size of vesicles more uniform (Dua, et al., 2012) (Laouini, et al., 2012) (Popovska, et al., 2013). The figure 4.1 shows this method step-by-step.
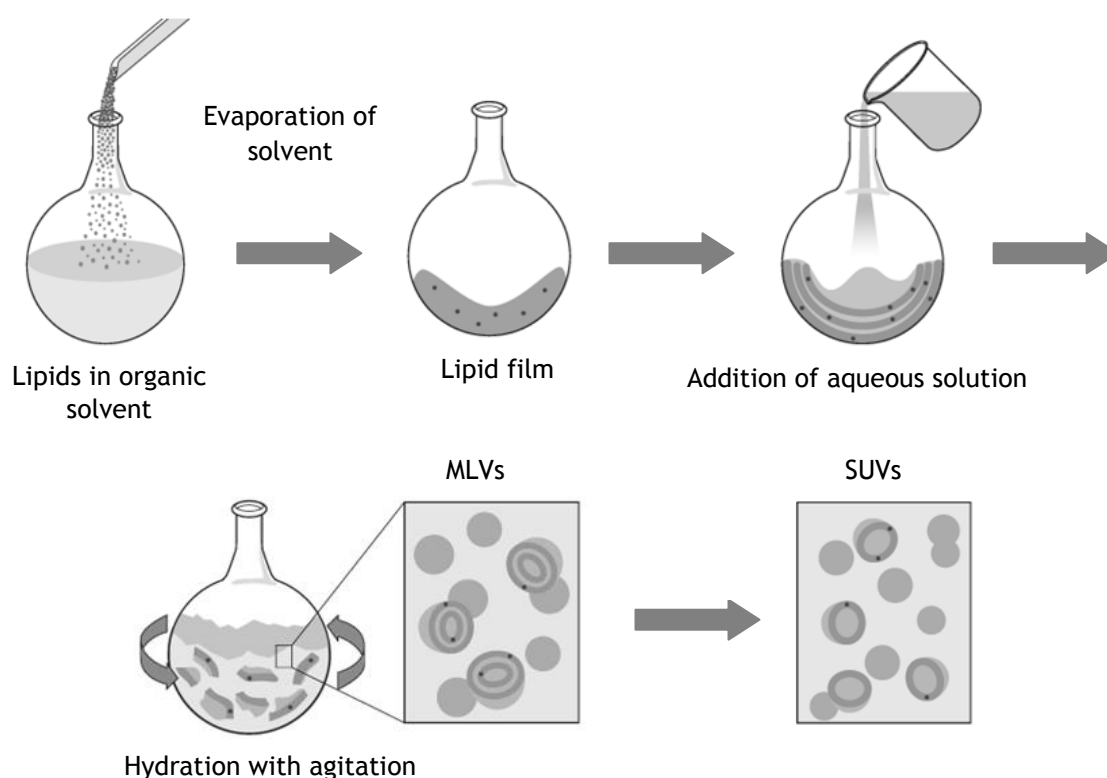
Figure 4.1 – Liposome production steps by method of hydration of a thin lipid film. Adapted from (Lasic, 1997).

Sonication is perhaps the most broadly used method for the preparation of SUVs (Akbarzadeh, et al., 2013). This method consist in disruption of MLVs suspensions using sonic energy (sonication) typically produces SUVs. The sonication of MLVs dispersion is accomplished by placing a test tube containing the suspension in a bath sonicator or placing the tip

of the sonicator in the test tube for 5 to 10 minutes above the Tm of the lipid (Dua, et al., 2012) (Sirisha, et al., 2012).

Lipid extrusion is a technique in which a lipid suspension is forced to pass through a polycarbonate filter with a defined pore size to yield particles having a diameter smaller, near the pore size of filter used (Lasic, 1997) (Sirisha, et al., 2012).

After the hydration is common perform the method of freezing and thawing of liposomes for increasing the trapped volume of drug. The freeze-thaw method is dependent on the ionic strength of the medium and the phospholipid concentration. It induces the physical disruption of lamellar structure leading to formation of LUVs. In general, the freeze and thawing cycles are repeated thirteen times (Akbarzadeh, et al., 2013) (Sirisha, et al., 2012).

For the production of liposomes, all the lipids were purchased from Avanti Polar Lipids (Alabama, USA): DSPC (1,2-distearoyl-*sn*-glycero-3-phosphocholine, MW 790.145), Chol (cholesterol ovine wool, MW 386.66), DSPE-PEG$_{2000}$ (1,2- distearoyl-*sn*-glycero-3-phosphoethanolamine-N-[amino(polyethylene glycol)-2000] (ammonium salt), MW 2790.49), POPC (1-palmitoyl-2-oleoyl-*sn*-glycero-3-phosphocholine, MW 760.10) and DOTAP (1,2-dioleoyl-3-trimethylammonium-propane (chloride salt), MW 698.55). The chemical structure of the phospholipids is shown in table 4.1. *Trans*-resveratrol (3,5,4'-trihydroxystilbene, purity ≥ 99%, MW 228.24) was purchased from Sigma-Aldrich (St. Louis, MO, USA).

Several approaches were used in order to encapsulate RES. All liposomes were prepared by the classic method of the lipid film hydration (Lasic, 1997). In the first approach, DSPC, Chol and DSPE-PEG$_{2000}$ were dissolved in chloroform (CF, MW 119.38, Sigma-Aldrich), at the molar ratio of 52:45:3. A lipid film was formed by evaporating the solvent through manual rotation under a nitrogen atmosphere. The nitrogen atmosphere allows rapid solvent evaporation and inhibits lipids oxidation. The film was held in a desiccant container overnight, to accomplish chloroform complete evaporation. The resultant dried lipid film was hydrated with 1.5 mL of a solution of RES in PBS buffer 7.4 (phosphate buffered saline, 10 Mm phosphate buffer, 2.7 mM potassium chloride and 137 mM sodium chloride, Sigma-Aldrich) at a molar ratio of 1:10 (RES: lipids moisture). The final lipid concentration was 0.8 mM and the RES concentration was 80 µM. After the lipid film was peeled off completely through vigorous shaking in a vortex (Vortex Genius 3, Ika®, Germany) for 15 minutes, to yield MLVs. In order to obtain LUVs, the suspension was submitted to ultrasounds in a sonicator bath (Ultrasonic cleaner, VWR®, Malasya) for 10 minutes, followed by extrusion through a polycarbonate membranes (Nuclepore Track-Etch Membrane, Whatman®, Maidstone, UK) with a specific pore size 11 times using an extruder (Mini-extruder, Avanti® Polar Lipids, Alabama, USA). The liposomes were then sequentially passed through membranes with pore diameters of 200 and 100 nm.

Table 4.2 shows the summary of the various approximations performed.

Table 4.1 - Chemical structure of the lipids used to prepared liposomes.
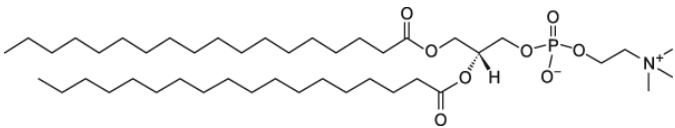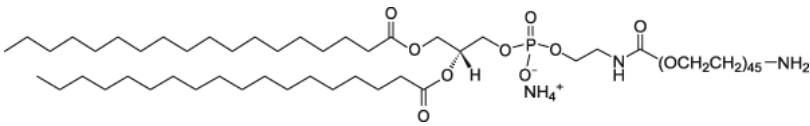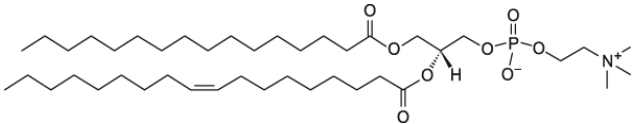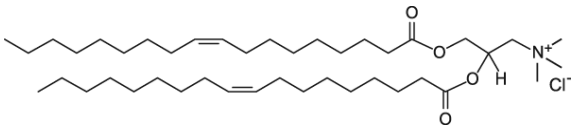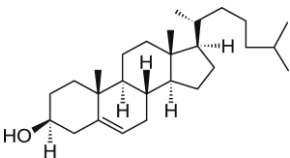
Chemical Structure	Names
	DSPC: 1,2-distearoyl-*sn*-glycero-3-phosphocholine
	DSPE-PEG$_{2000}$: 1,2-distearoyl-*sn*-glycero-3-phosphoethanolamine-N-[amino(polyethylene glycol)-2000]
	POPC: 1-palmitoyl-2-oleoyl-*sn*-glycero-3-phosphocholine
	DOTAP: 1,2-dioleoyl-3-trimethylammonium-propane
	Cholesterol

Table 4.2 - Summary of the several approaches performed for production of liposomes.

		Approaches											
		1	2	3	4	5	6	7	8	9	10	11	12
Lipids	DSCP	✓	✓	✓	✓	✓	✓	✓	✗	✗	✗	✗	✗
	Chol	✓	✓	✓	✓	✓	✓	✓	✓	✓	✓	✓	✓
	PEG	✓	✓	✓	✓	✓	✓	✓	✓	✗	✗	✗	✗
	POPC	✗	✗	✗	✗	✗	✗	✗	✓	✓	✗	✓	✗
	DOTAP	✗	✗	✗	✗	✗	✗	✗	✗	✗	✓	✗	✓
Molar ratio (lipid:Chol:PEG)		52:45:3	52:45:3	52:45:3	52:45:3	52:45:3	52:45:3	52:45:3	52:45:3	55:45	55:45	10:1	10:1
Organic solvent		CF	CF	CF	CF	CF	CF	CF	CF	EtOH	EtOH	EtOH	EtOH
Molar ratio (RES: lipids moisture)		1:10	1:20	1:100	1:10	1:10	1:10	1:10	1:10	1:4	1:4	1:4	1:4
Final lipid concentration		0.8 mM	1.6 mM	8 mM	0.8 mM	0.8 mM	0.8 mM	0.8 mM	0.8 mM	80 mM	80 mM	80 mM	80 mM
RES concentration		80 µM	80 µM	80 µM	80 µM	80 µM	80 µM	80 µM	80 µM	20 mM	20 mM	20 mM	20 mM
Addition of RES	Organic phase	✗	✗	✗	✓	✓	✗	✗	✗	✓	✓	✓	✓
	Aqueous phase	✓	✓	✓	✗	✗	✓	✓	✓	✗	✗	✗	✗
drug solution solvent		PBS	PBS	PBS	CF	EtOH	10% (v/v) DMSO in water	2% (v/v) EtOH in water	water	EtOH	EtOH	EtOH	EtOH
Freezing/unfreezing cycles		✗	✗	✗	✗	✗	✗	✓	✓	✓	✓	✓	✓
Extrusion		✓	✓	✓	✓	✓	✓	✓	✓	✗	✗	✗	✗

4.1.2 – PLGA Nanoparticles Preparation

Several methods have been devised to synthesize PLGA NPs depending on the physic-chemical characteristics of the drug to be encapsulated. The characteristics of the obtained NPs, as size and structural organization, depend upon the chosen method and solvents (Kumari, et al., 2010) (Makadia & Siegel, 2011). The most common methods are single or double-emulsion solvent evaporation and nanoprecipitation (Kumari, et al., 2010). While nanoprecipitation is suitable for the entrapment of both hydrophobic and hydrophilic drugs (Schubert, et al., 2011), the choice of single or double emulsion depends upon the hydrophilicity of the drug to be encapsulated (Makadia & Siegel, 2011). Single-emulsion is a suitable choice for encapsulating hydrophobic drugs, and double-emulsion is mostly used for hydrophilic drugs (Danhier, et al., 2012) (Makadia & Siegel, 2011).

The technique used in this work was the emulsification-solvent evaporation technique. This process involves oil-in-water (o/w) emulsification. Polymer in the appropriate amount is first dissolved in a water immiscible, volatile organic solvent in order to prepare a single phase solution. The drug is then added to the polymer solution to produce a solution or dispersion of the drug particles. This polymer dissolved drug dispersed solution is then emulsified in a larger volume of water in presence of an emulsifier to yield an o/w emulsion. The emulsion is then subjected to solvent removal by either evaporation or extraction process to harden the oil droplets. The solid microspheres so obtained are then washed and collected by filtration, sieving, or centrifugation (Hans & Lowman, 2002) (Jain, 2000) (Makadia & Siegel, 2011) (Vasir & Labhasetwar, 2007) (Wischke & Schwendeman, 2008).

For PLGA NPs preparations, PLGA Resomer® RG503H (50:50; MW 24.000 – 38.000), *trans*-resveratrol (purity ≥ 99%, MW 228.24), ethyl acetate (MW 88.11), acetone (MW 58.08) and Pluronic® F-127 were purchased from Sigma–Aldrich (St. Louis, Mo., U.S.A). Extracts of the grape seed and grape skin (purity ≥ 95%) was purchased from Monteloeder (Elche, Alicante, Spain). Two aqueous solutions of 0.1% and 1% (w/v) Pluronic F-127 were prepared in deionized and filtered ultrapure Milli-Q water (Milli-Q Academic, Millipore, France).

To synthesize PLGA NPs, two experimental conditions were tested. In the first experimental condition, 100 µl solution of 100 mg/ml of PLGA in ethyl acetate was prepared and RES (36.52 µg), extracts of grape seed (0.77 mg) and skin (0.96 mg) were added. In the second experimental condition, the drugs were dissolved in 50 µl of acetone and added at 100 µl solution of 100 mg/ml of PLGA in ethyl acetate. Then, 200 µL of an aqueous solution of 1% (w/v) pluronic F-127 was added dropwise to the organic phase. The moisture was vortexed (Genius 3, ika®vortex, Germany) for 30 seconds and emulsified by sonication for 5 minutes in a beaker with ice using Ultrasonic cleaner (VWR™, Malaysia). Typically, stirring of the emulsion originates microdroplets. In order to induce the nanosized droplets, sonication process was carried out. The size reduction is induced through a two-step mechanism. Firstly, applying acoustic waves through the water creates interfacial waves and instability, which causes the eruption of the oil phase into the water medium in the form of droplets. Secondly, applying low frequency ultrasound causes acoustic cavitation, that is, the formation and subsequent collapse of microbubbles, leading to turbulence. This turbulence breaks up the primary droplets of dispersed oil into nanosized droplets (Jafari, et al., 2006) (Kentish, et al., 2008).

After emulsification completed, the emulsion was poured rapidly into 2.5 ml of 0.1% (w/v) pluronic F-127 and stirred (800 rpm) at 70ºC for 10 minutes in order to completely evaporate the organic solvent and ensure complete dissolution of the drugs, using MR 3001 K series mag-

netic stirring hotplate (Heidolph, Germany). The evaporation step was performed in a flow chamber SterilGARD®e³ from The Baker Company (Sanford, USA). It is important to note that, this transfer step must be completed very quickly, in order to avoid PLGA NPs aggregation before being stabilized by the surfactant (Li, et al., 2008).

The resulting suspension was filtered with Millex-GP Filter Units (0.2 µm, polyethersulfone) (Millipore Express, Ireland) and incubated at 4°C overnight to avoid NPs aggregation and increase their stability. Then the NPs were collected by centrifugation (14500 rpm for 30 minutes) with MiniSpin®plus (Eppendorf, Germany), and the pellet was resuspended in ultrapure water and stored for analysis.

4.1.3 – Encapsulation Efficiency of Liposomes

The first step for the determination of the encapsulation efficiency is the separation between the encapsulated and free drug. Several separation techniques have been described in the literature (Laouini, et al., 2012) (Popovska, et al., 2013) (Vanaja, et al., 2013). Free RES was removed from liposome dispersions by two techniques, dialysis and gel-permeation chromatography.

In the first technique, the separation between the free RES and the encapsulated RES was performed using a dialysis membrane with an approximate molecular weight cut-off (MWCO) of 100 kDa (Spectra/Por® Float-A-Lyzer® G2, Spectrum Laboratories, USA). Initially, the membrane was submerged overnight in ultra-pure water to remove glycerin and achieve maximum permeability. Then, 500 µl of sample was placed into dialysis bag. The liposomal suspension was dialysed against 6 ml of PBS for 2h30 at 4°C. The medium of dialysis was replaced every 5 minutes.

To study the efficiency of encapsulation using the second technique, PD MiniTrap™ G-25 column contain Sephadex™ G-25 Medium (GE Healthcare, Uppsala, Sweden) was used to separate free RES from liposomes. Free RES and liposomes were separated through gravity protocol based on their different sizes. As liposomes are larger than the pores of column, they are excluded and therefore eluted. Unloaded liposomes suspension and solution of RES were also submitted to this separation process as a control. Depending on the hydration solution used in preparation of the liposomes the column was equilibrated with 8 ml of ultra-pure water or PBS and then 0.5 ml of liposomes suspension was added to the column. As the sample entered the packed bed completely, it was eluted and collected with 1.0 ml of PBS.

After the separation, to quantify the amount of RES encapsulated, the liposomes were burst with sodium dodecyl sulphate (SDS, MW 288.38, Sigma-Aldrich, Germany), in a 25:75 (v/v) proportion (liposomes: SDS) and their absorbance was measured using BioTek® Synergy 2 Multi-Mode Reader.

The encapsulation efficiency (EE%) is defined as the ratio between the amount of resveratrol encapsulated in liposomes and the amount of resveratrol used for the preparation following equation (Isailović, et al., 2013) (Lu, et al., 2012):

$$EE\% = \frac{\text{Amount of drug encapsulated}}{\text{Amount of used drug}} \times 100. \quad\quad (4.1)$$

4.1.4 – Encapsulation Efficiency, Loading Capacity and Process Yield of PLGA NPs

To quantify the amount of RES and seed and skin grape extracts encapsulated in the NPs, the NPs suspensions were centrifuged (14500 rpm for 30 minutes) and the supernatants analyzed. The samples were measured by UV-Vis spectrophotometry at 305 nm, using a UV-1700 PharmaSpec UV-VIS Spectrophotometer Shimadzu (Japan). The results were correlated to calibration curve (Figure 3.3). Encapsulation efficiency (EE%) of PLGA NPs was calculated by the following equation:

$$EE\% = \frac{total\ weight\ of\ drug - unloaded\ weight\ of\ drug}{total\ weight\ of\ drug} \times 100. \qquad (4.2)$$

RES, seed and skin grape extracts loading capacity (LC%) of PLGA NPs was calculated by the following equation:

$$LC\% = \frac{total\ weight\ of\ drug - unloaded\ weight\ of\ drug}{total\ weight\ of\ polymer} \times 100. \qquad (4.3)$$

The process yield (PY%) of NPs was calculated by comparing the quantity of polymer and drug initially taken for the production process, and the quantity of the NPs finally obtained. The yield of the process was calculated by the following equation:

$$PY\% = \frac{total\ nanoparticles\ weight}{total\ weight\ of\ polymer + total\ weight\ of\ drug} \times 100. \qquad (4.4)$$

To determine the NPs weight, the NPs suspension was centrifuged (14500 rpm for 30 minutes). The pellet NPs were resuspended in 200 µl of deionized water and the supernatant was discarded. The pellet was dried overnight, and the final mass of the NPs was measured.

4.1.5 – Stability Studies

In order to evaluate the PLGA NPs stability, PLGA NPs' dispersions in ultrapure water were stored at 4 °C. These tests were performed in all formulations prepared (unloaded-PLGA NPs, RES-loaded, grape seed extract-loaded and grape skin extract-loaded NPs, for the two experimental conditions). The stability of the PLGA NPs was analyzed through the size and zeta potential variation. These measurements were performed every day, over a period of 1 month.

The size was measured by dynamic light scattering (DLS) technique at RT. Zeta potential was also measured for the same samples by the laser Doppler velocimetry method. The measurements were performed in a ZetaSizer Nano ZS (Malvern instrument, Worcesterchire, UK).

4.1.5.1 – Zeta Potential

The overall charge that a particle acquires in a particular medium is called zeta potential. Any particle in suspension exhibits this physical property. Measurements of zeta potential are

commonly used to study the stability of colloidal systems. If the particles in suspension have a large zeta potential (negative or positive) they will tend to repel each other and there will be no tendency to aggregation. However, if the particles have low zeta potential values there will be no force to prevent the particles flocculating. To measure the zeta potential, the particles are illuminated by a laser that provides a light source. When an electric field is applied to the cell, any particles moving through the measurement volume will lead to fluctuation of the detected light with a frequency proportional to the particle speed. This information is transmitted to a digital signal processor and the potential zeta is calculated. Particles suspension normally are considered stable with zeta potentials greater than +30 mV or less than −30 mV (Laouini, et al., 2012) (Popovska, et al., 2013).

The zeta potential of dispersed colloidal particles can be measured by electrophoresis. The electric force causes the particle to move in relation to a stationary liquid at a constant velocity. The ratio of the velocity to the electric field E is the electrophoretic mobility, μ_E. The mobility is converted into zeta potential, ζ, using the Smoluchowski equation:

$$\zeta = \frac{\eta \mu_E}{\varepsilon} \tag{4.5}$$

where η is the viscosity of the solution and ε is the permittivity of the solution (Laouini, et al., 2012) (Popovska, et al., 2013).

In this work, ZetaSizer Nano ZS (Malvern Instruments, Worcesterchire, UK) was used to measurements of zeta potential of the NPs in suspension. It was used folded capillary cells from Malvern (Worcesterchire, UK) and the dispersant medium was water. Mean values for each preparation were obtained by duplicate measurements. Each measurement was performed with 10 runs.

4.1.5.2 – Dynamic Light Scattering

Dynamic Light Scattering (DLS), also referred to as quasi-elastic light scattering, is a NPs characterization technique since it enables the determination of particles size and size distribution in dispersions. The method is based on the fluctuations in the intensity of light scattered by a small volume of a solution in the microsecond time range which are directly related to the Brownian motion of the solute (Berne & Pecora, 1976). Submicrometer size particles in suspension exhibit significant random motion because of collisions with the molecules of the surrounding liquid medium called Brownian motion. As the result, when light irradiates a colloidal dispersion, the phases of the scattered waves fluctuate randomly in time. The scattered light intensity from individual particles interfere with each other, and hence the net intensity of the scattered light fluctuates randomly in time (Boyd, et al., 2011) (Jiang & Oberdorster, 2009).

Diffusion is controlled by temperature (the higher the temperature, the faster the movement), viscosity (the higher the viscosity, the slower the movement) and NPs size (the bigger the NPs, the slower the movement). Since the solvent and temperature during measurements are known and constant, it is possible to relate the variation of scattered light intensity to the NPs size (Jiang & Oberdorster, 2009). The Stokes-Einstein equation is used to determine NP size:

$$R_H = \frac{kT}{6\pi\eta D} \; , \tag{4.6}$$

where R_H is the hydrodynamic radius, k is the Boltzmann constant, T is the absolute temperature, η is the viscosity of the medium and D is the diffusion coefficient.

This relation is the basis of the particle size determination by DLS, but it is valid only for monodisperse particles. This measured size value refers to the hydrodynamic radius (HR). HR represents the size of a hypothetical sphere that moves the same way as the particle that is being measured, i.e. HR represents the NPs and its solvation shell. Therefore HR will always be slightly than the real radius of the NPs. This solvation shell depends on the solvent, whereby successive measurements must always use the same solvent (Boyd, et al., 2011) (Jiang & Oberdorster, 2009).

In addition to the size, DLS also allows to determine the Polydispersity Index (PdI). PdI is an indicative of the heterogeneity of sizes of NPs in a suspension. A solution is monodisperse if the NPs have the same size. In this case, the PdI is less than 0.1. On the contrary, if the NPs have an inconsistent size, the dispersion is called a polydispersion. The presence of aggregates can distort the results, since the equipment analyze them as single particle of bigger size, resulting in higher PdIs (Jiang & Oberdorster, 2009).

In this work, DLS measurements also were performed using a ZetaSizer Nano ZS (Malvern Instruments, Worcesterchire, UK). The size distribution was given by PdI. All the determinations were performed in disposable cells (Sarstedt, Germany) and using water as dispersant medium. Mean values for each preparation were obtained by triplicate measurements. Each measurement was performed with 12 runs.

4.1.6 – Morphologic Analysis of PLGA NPs

The morphological examination of the NPs was performed by transmission electron microscopy.

4.1.6.1 – Transmission Electron Microscopy

Transmission electron microscopy (TEM) is arguably one of the most efficient and versatile tools for the characterization of nanomaterials morphology because gives real space images, including the surface and the internal structures of materials, tissues and cells. This microscopy has much higher resolution than conventional light microscope and is based on the principle of electron wave–particle duality. As electron is a charged particle it can be accelerated in an electric field, and its trajectory can be deflected by electric and magnetic fields. As this accelerated electron also behave like wave, it is possible to control its wavelength by potential differences. The wavelength depends of velocity, as can be verified in the following equation:

$$\lambda = \frac{h}{m\,v} \; , \tag{4.7}$$

where λ is the electron wavelength; h, the Planck's constant; m, the electron mass; and v, the electron velocity. Therefore, depending on the accelerating voltage used, it is possible to choose the wavelength of the electron beam. The higher the accelerating voltage, the shorter the wavelength (Asadabad & Eskandari, 2015).

TEM is a microscopy technique wherein a beam of electrons is applied and is accelerated by an electric field formed by a voltage difference of, typically, 200 kV. The set of condenser lenses focus the electron beam on strong magnetic fields to a spot on the sample to be investigated. Then the beam hits the sample and the electrons interact with the mater. Depending on the density of the sample, some of the electrons are scattered and some of them are transmitted through the sample. An image is formed from the electrons transmitted through the specimen, magnified and focused on an objective lens, and appears on an imaging screen (Figure 4.2) (Wang, 2000).
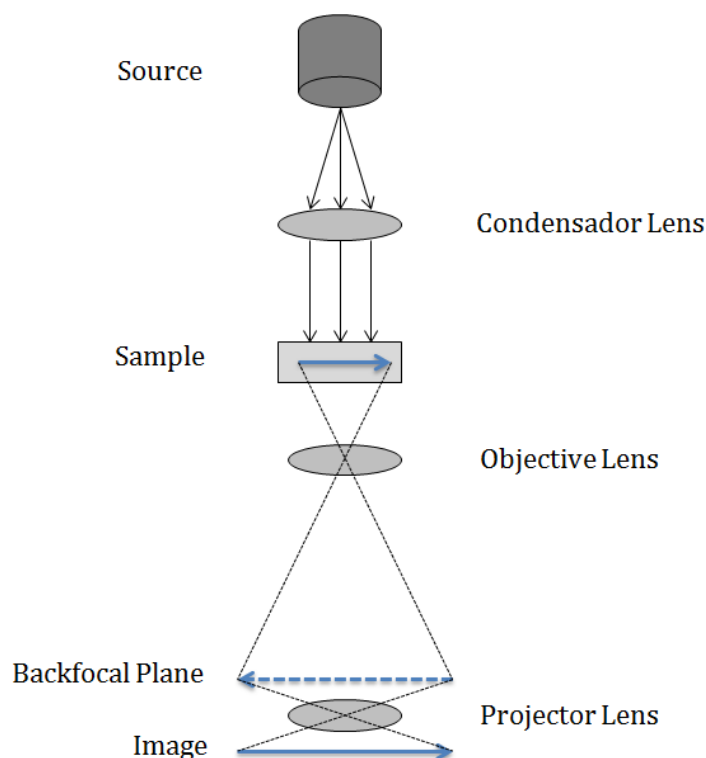
Figure 4.2 – Image formation in transmission electron microscope. Adapted from (Cahn & Haasen, 1996) (Hiemenz & Rajagopalan, 1997).

The objective diaphragm ensures the exclusion of inelastically scattered electrons in order to enhance the image contrast. The beam that reaches the phosphor screen has different amounts of electrons that pass through particular regions of the sample. This difference is responsible for the image contrast. Darker areas of the image represent the regions of the sample through which fewer electrons were transmitted, due to the greater thickness or density. Contrariwise, brighter areas are the result of increased electronic transmission through the sample, i.e. representing thin regions of the sample (Asadabad & Eskandari, 2015).

TEM was used to the morphological examination of the PLGA NPs. For that purpose, 5 µl of each sample was placed on carbon-formvar coated 200-400 mesh spacing grids (Agar Scientific, UK) and let to adsorb for 5 minutes. The negative staining was performed with 2% (w/v) filtered aqueous solution of uranyl acetate for 45 seconds. The uranyl acetate solution was centrifuged at 12000 rpm for 3 minutes to pellet any unsolubilized uranyl acetate before use. After removing the excess of the negative staining solution and drying the grids, the samples were visualized using a Jeol JEM 1400 (Tokyo, Japan) electron microscope at 80 kV.

4.2 – Results and Discussion

4.2.1 – Encapsulation Efficiency of Liposomes

Two techniques were used to remove free RES from liposome dispersions, dialysis and gel-permeation chromatography, and thus calculate the encapsulation efficiency. In all approaches conducted, after separating the free RES from liposome dispersions and after bursting liposomes with SDS, was not detected the characteristic peak of RES indicating that this was not encapsulated.

The results of figure 4.3 demonstrated that after removing the free RES from liposome dispersions (Figure 4.3 b)), RES was not detected. This does not indicate in advance that the RES was not encapsulated because what was encapsulated cannot be detected within the liposomes. Therefore, the liposomes were busted with SDS, but RES was not detected (Figure 4.3 c)). The results of figure 4.3 are relative to the first approach performed, but the same results were obtained for the others approaches.

Some studies confirmed the difficulty of encapsulating RES in liposomes. Neves, et al. described the RES as potentially able to perturb membrane phospholipids possibly impairing or altering their structural and role (Neves, et al., 2012). The studies of Cao, et al. demonstrated that RES is located preferably in the liposome surface (Cao, et al., 2009). Bonechi, et al. also demonstrated that the RES was associated to the surface of the liposomes and not penetrated inside the liposomes (Bonechi, et al., 2012). Selvaraj, et al. concluded through their studies that stilbenes preferentially interact with the polar headgroups of the lipids. The authors showed that RES interacts with the lipid headgroup region of the bilayer and that RES is located at the superficie of liposomes (Selvaraj, et al., 2013).

So, this system for the encapsulation of RES- and extracts-loaded in liposomes was dropped.

4.2.2 – Encapsulation Efficiency, Loading Capacity and Process Yield of PLGA NPs

The obtained results for encapsulation efficiency (EE%) for both experimental conditions are expressed in percentages in table 4.3. EE% values achieved are according to our experience with other hydrophobic drugs (Frasco, et al., 2014) and other results reported in literature that state that EE values for PLGA NPs may vary from 6 to 90% (Danhier, et al., 2012). One reason for not having reached the higher values may be related to drug solubility in the surfactant solution (Hans & Lowman, 2002). As already reported in other studies, drugs can be incorporated into the core of the micelles formed by pluronic (Fessi, et al., 1989). As table 4.3 shows, no significant changes of EE values (P>0.05) were observed for the both experimental conditions for the encapsulation of the extracts. However for encapsulation of RES, the obtained values significantly increased (P≤0.05) with the second experimental condition, from 68±8 % to 80±6 %. This can be explained by better dissolution of resveratrol in acetone (Sun, et al., 2008). As RES showed a higher EE% the second experimental condition was selected for the following experiments.
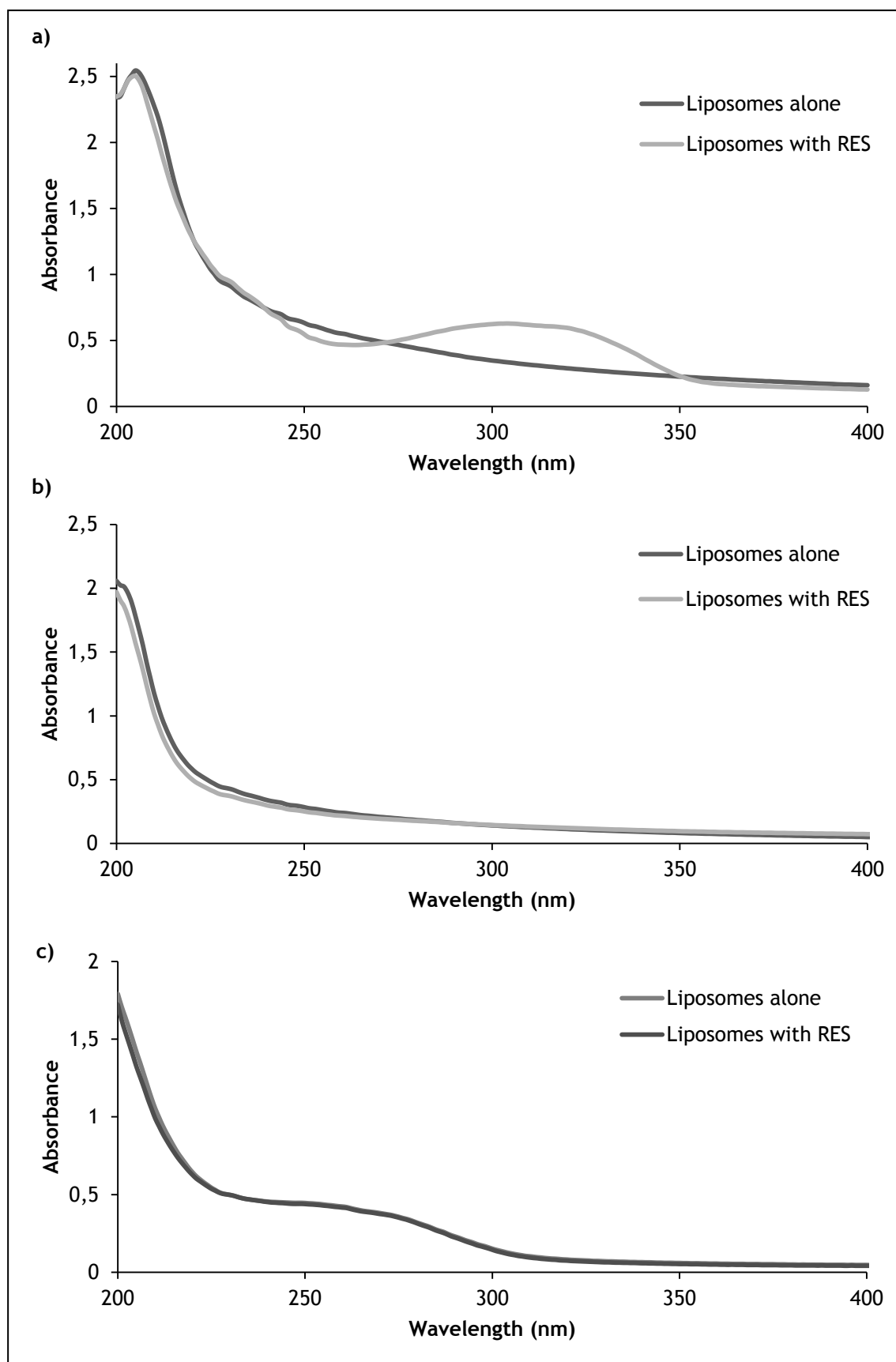
Figure 4.3 – UV-spectrum of liposomes alone and liposomes with RES **a)** before the separation of free RES, **b)** after the separation of free RES and **c)** busted with SDS after the separation of free RES.

Table 4.3 – Encapsulation efficiency values for both experimental conditions performed. In the first condition ethyl acetate was used for dissolving the drugs and in the second condition was used acetone. Data represented as mean ± SD (n=3).

	EE%		
	RES-loaded PLGA NPs	**Grape seed extract-loaded PLGA NPs**	**Grape skin extract -loaded PLGA NPs**
1st experimental condition	68±8	74±3	73±9
2nd experimental condition	80±6	75±5	74±8

The loading capacity of PLGA NPs was also evaluated. As expected, loading capacity values increased significantly ($P \leq 0.05$) with the extracts-loaded PLGA NPs in comparison with RES-loaded PLGA NPs (Table 4.4). RES-loaded NPs exhibited a loading capacity of 0.29±0.05 %, and the NPs loaded with grape seed and skin extracts have a loading of 5.8±0.4 % and 7.1±0.8 %. This was already expected due to the reduced amount of RES used for preparing the PLGA NPs. PLGA NPs normally exhibit poor loading capacity (around 1% which means that NPs content 1 mg active ingredient per 100 mg polymers of NPs) (Danhier, et al., 2012). Thus, the values obtained in this experimental work are supported by the ones found in the literature as also by our experience with other hydrophobic drugs (Frasco, et al., 2014).

The yield of this PLGA NPs production process is quite low with values of 3.4±0.4 % for RES-loaded PLGA NPS, 5.2±0.5 % for grape seed extract-loaded PLGA NPs and 6.6±0.7 % for grape skin extract-loaded PLGA NPs (Table 4.4). The values obtained in this experimental work are supported by other experiences that used acetone with solvent for de PLGA NPs preparation and a very low ratio between the drug and polymer (Murakami, et al., 1999).

Table 4.4 – Loading capacity and process yield values for loaded PLGA NPs. Data represented as mean ± SD (n=2).

	RES-loaded PLGA NPs	**grape seed extract-loaded PLGA NPs**	**grape skin extract -loaded PLGA NPs**
LC%	0.29±0.05	5.8±0.4	7.1±0.8
PY %	3.4±0.4	5.2±0.5	6.6±0.7

4.2.3 – Stability Studies of PLGA NPs

The single emulsion solvent evaporation method allowed the encapsulation of RES, grape seed extract and grape skin extracts in the PLGA NPs. The attained results for mean diameter, PdI and zeta potential, for the PLGA NPs loaded with RES, grape seed extract and grape skin extracts are shown in table 4.5.

As it can be concluded after the analysis of table 4.5, the mean diameters of the loaded PLGA NPs ranged from 158 to 182 nm. That is, they were according to the expected values

because according with literature, PLGA NPs size is founded to be in the range of 100 to 250 nm (Danhier, et al., 2012). As it is also shown in table 4.5, drug-loaded NPs exhibited a significantly larger size than unloaded PLGA NPs (P≤0.05), regardless of whether it was encapsulated RES, grape seed extract or grape skin extracts. The size increased from 161 ± 3 nm to 179 ± 3 nm, 178 ± 2 nm and 175 ± 1 nm, respectively. This effect was reported in studies that argue that the drug causes an expansion of the polymeric matrix, increasing particle size (Musumeci, et al., 2006). The prepared systems exhibited a narrow size distribution (PdI ≤ 0.1).

Table 4.5 – Physicochemical features of RES, grape seed extract and grape skin extract-loaded PLGA NPs. Data represented as mean ± SD (n=2).

PLGA NPS	Mean Diameter (nm)	PdI	Zeta Potential (mV)
Unloaded	161±3	0.05±0.03	- 31±2
RES-loaded	179±3	0.09±0.02	- 26±2
Grape seed extract-loaded	178±2	0.05±0.03	- 28±1
Grape skin extract -loaded	175±1	0.06±0.01	- 26±1

Zeta potential values for PLGA NPs are negative as expected, ranging from -33 to -24 mV, due to their carboxylic end-groups, as it is shown in table 4.5. Zeta potential absolute value significantly decreased from 31.2 mV in unloaded PLGA NPs to 26.1, 27.5 and 26.4 mV in RES-loaded, grape seed extract-loaded PLGA NPs and grape skin extract-loaded PLGA NPs respectively (P≤0.05). These values could be explained by drug adsorption on PLGA NPs surface.

As already reported by Musumeci, et al., the drug adsorbed on PLGA NPs surface exert a masking effect of the superficial carboxylic groups, reducing the effective NP charge (Musumeci, et al., 2006). This masking effect could also explain the decrease, although not significant (P>0.05), in zeta potential values. Moreover, zeta potential values were not significantly different between the drugs used for preparation NPs (P>0.05).

In order to study the stability of the PLGA NPs over time, their mean diameter, PdI and zeta potential values were measured during 1 month. Stability tests are presented in table 4.6. Mean size variation is expressed in terms of ratio S_t/S_i.

Over this time, there were no significant variations on these parameters, which indicate that the PLGA NPs are stable. It is very important to certify that the vesicles are not aggregated, since the size and stability of PLGA NPs are critical for their cell internalization. RES-loaded NPs exhibited a mean S_t/S_i value of 0.993 for approximately 1 month, while grape seed extract-loaded presented a value of 1.01 and grape skin extract-loaded of 1.03. The monodisperse RES-, grape seed extract- and grape skin extract-loaded PLGA NPs showed mean sizes of 179±2 nm, 181±4 nm and 176±1 nm, respectively, which have remained constant over time. The size distribution (PDI≤ 0.1) of all preparation indicates the formation of uniform

structures. These data proves that the NPs remained physically stable at storage conditions (4 ℃) for approximately 1 month.

Zeta potential values showed a slight decrease (no significantly different (P>0.05)) over time (table 4.6). However as applying an electric field to the sample may alter it, only values for size were considered for stability evaluation purposes.

Table 4.6 – Zeta potential, mean diameter and PdI values for loaded PLGA NPs, over a period of 1 month. Mean size variation is expressed in terms of ratio S_t/S_i, where S_t is mean diameter after t days of storage and Si is the NPs initial mean size. Data represented as mean ± SD (n=3 for mean diameter and PdI and n=2 for zeta potential). These data is only relative to one batch for each formulation, loaded and unloaded.

PLGA NPs	Mean diameter (nm)	Ratio S_t/S_i	PdI	Zeta Potential (mV)
RES-loaded				
Day 1	179 ± 2 nm	-	0.039 ± 0.021	-26.1 ± 1.8 mV
Day 7	175 ± 4 nm	0.978	0.042 ± 0.012	-25.1 ± 0.8 mV
Day 14	177 ± 6 nm	0.989	0.056 ± 0.029	-22.5 ± 0.3 mV
Day 28	181 ± 5 nm	1.011	0.075 ± 0.015	-21.8 ± 0.7 mV
Grape seed extract-loaded				
Day 1	181 ± 4 nm	-	0.065 ± 0.024	-24.6 ± 0.9 mV
Day 7	185 ± 3 nm	1.022	0.034 ± 0.014	-23.9 ± 0.5 mV
Day 14	182 ± 9 nm	1.006	0.047 ± 0.017	-23.5 ± 1.1 mV
Day 28	183 ± 2 nm	1.011	0.056 ± 0.019	-22.4 ± 0.7 mV
Grape skin extract-loaded				
Day 1	176 ± 1 nm	-	0.056 ± 0.014	-26.4 ± 0.3 mV
Day 7	177 ± 1 nm	1.011	0.055 ± 0.020	-25.9 ± 0.1 mV
Day 14	183 ± 5 nm	1.046	0.037 ± 0.018	-23.5 ± 0.3 mV
Day 28	182 ± 3 nm	1.040	0.046 ± 0.017	-24.5 ± 0.9 mV

4.2.4 – Morphologic Analysis of PLGA NPs

TEM analysis of PLGA NPs revealed spherical and uniform shaped NPs, as it is shown in figure 4.4. The diameter of the NPs is in conformity with the size measurement by DLS. These images also show a relatively monodisperse NPs.

NPs' stability is a result of the electrostatic forces due to the PLGA carboxylate groups at the NP surface, and the surfactant behavior that also plays a crucial role in maintaining nanosuspension stabilization. During particle formation, the stabilizer is able to modify NPs stabilization (Trump, et al., 2010) by adsorbing onto the NP surface (Wolpin, et al., 2012). In

fact, in figure 10, a morphologic examination performed by TEM shows a pluronic layer surrounding PLGA NPs. The surfactant causes steric repulsions forming a mechanic barrier prohibiting droplet approaching. Thermodynamic stabilization can also be considered, due to a loss of configurational entropy of surface adsorbed pluronic when overlapping occurs for approaching droplets (Wilczewska, et al., 2012). For all those reasons, it can be concluded that the method followed for the preparation of PLGA NPs produced well-stabilized monodisperse NPs.
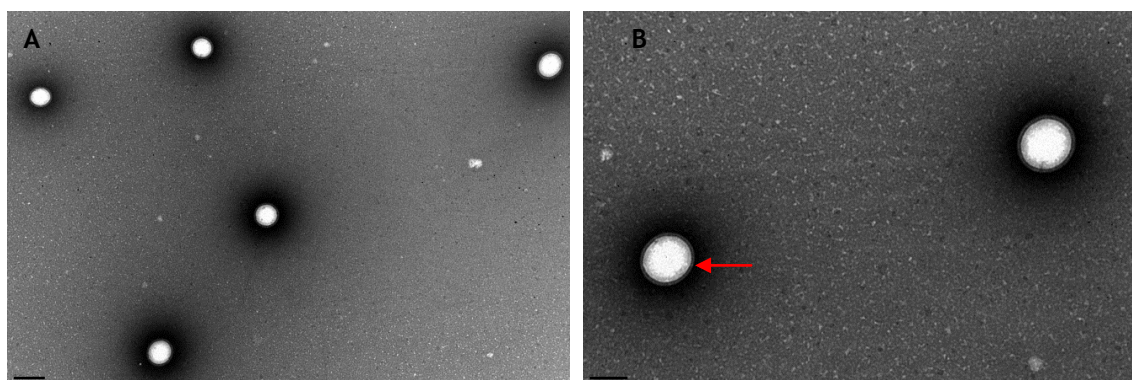
Figure 4.4 – TEM images of unloaded PLGA NPs. The scale bars correspond to (A) 200 nm and (B) 100 nm. The red arrow indicates the pluronic layer surrounding the PLGA NPs.

Chapter 5

Interaction of Aβ with Resveratrol and Extracts of Grape Seed and Skin

The aggregation process of the Aß peptide leads to the formation of insoluble fibrils which accumulate in senile plaques, deposits that characterize AD (Clippingdale, et al., 2001) (Klafki, et al., 2006) (Selkoe, 2001). The more abundant sequences of the peptide have 40 (~90%), Aß$_{(1-40)}$, and 42 (~10%), Aß$_{(1-42)}$, amino acids (Lee, et al., 2004). The peptide with 42 amino acids is more toxic ant it is the major component of the neuritic plaques found in AD (Hardy & Selkoe, 2002) (Lee, et al., 2004). The smaller aggregated intermediates, the Aß oligomers, are considered the more toxic species (Hardy & Selkoe, 2002). The imbalance between Aß production and its clearance leads to the Aß aggregation in the brain, that plays a key role in the development of AD (Li, et al., 2012).

Insoluble fibrillar protein aggregates are considered a pathological feature of several neurodegenerative diseases. Protein misfolding or partially folded structure is responsible for the fibrillation of various amyloidogenic proteins/peptides (Ahn, et al., 2007). Thus, it is essential to find molecules that prevent or interrupt the aggregation of proteins (Feng, et al., 2009). Various natural compounds have been suggested as therapeutics for AD and PD. Among these compounds, RES arouses great interest (Amri, et al., 2012). Several studies have demonstrated that RES is capable of preventing a variety of disorders, including cardiovascular diseases, cancer, diabetes, arthritis and neurodegenerative diseases. Given the benefits of RES, it is believed that it is useful in the therapy of AD and PD (Gusman, et al., 2001). RES has anti-amyloidogenic activity because it promotes the intracellular degradation of Aß by a mechanism involving the proteasome, thereby reducing levels of Aß (Marambaud, et al., 2005).

This chapter relates to the interaction between different drugs (RES and extracts of grape seed and skin) and Aß peptide.

5.1 – Material and Methods

5.1.1 – Amyloid-Beta Peptides

Aß$_{(1-42)}$ (amyloid-ß peptide 1-42, purity > 95%, MW 4514.14) was purchased from Selleck Chemicals (Houston, Texas, USA) (Figure 5.1). The aggregation state and the structure of the peptide are highly dependent on the sample batch (Soto, et al., 1995). To improve peptide solubility and disaggregate pre-formed agglomerates, the peptide was dissolved in 100% 1,1,1,3,3,3- hexafluoro-2-propanol (HFIP, purity ≥ 99.8%, Sigma-Aldrich, Germany) at 1 mg/mL concentration and kept at room temperature for 1–2 h. HFIP was evaporated with nitrogen flow and under vacuum. The peptide film with the Aß$_{(1-42)}$ in a monomeric structure was dissolved in dimethyl sulfoxide for molecular biology (DMSO, purity ≥ 99.9%, MW 78.13, Sigma-Aldrich, Germany) at 9 mg/mL concentration. Aß$_{(1-42)}$ solution is stored at -20 ˚C (Nilsson, 2004) (Rocha, et al., 2009) (Sabaté & Estelrich, 2005).
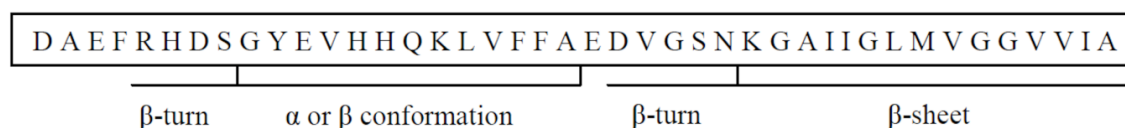
Figure 5.1 – Amino acids of the Aß peptide used in this study and their secondary structure prediction.

5.1.2 – Stock Solutions of Resveratrol, extracts of grape seed and skin and loaded-PLGA NPs

Stock solutions of RES (purity ≥ 99%, MW 228.24, Sigma-Aldrich) and extracts of the grape seed and grape skin (purity ≥ 95%, Monteloeder) were prepared as is described in the Chapter 3, Section 3.1.1.

Stock solutions of loaded-PLGA NPs were prepared as is described in the Chapter 4, Section 4.1.2.

5.1.3 – Fluorescence Measurements

Fluorescence occurs when a molecule absorbs light photons from the UV-visible light spectrum (200-900 nm), known as excitation, causing transition to a high-energy electronic state, and then rapidly emits light photons as it returns to its ground state, in less than 10^{-9} seconds. The processes that occur between the absorption of light and its emission are represented conveniently in the Jablonski diagram (Figure 5.2) (Lakowicz, 1988) (So & Dong, 2002).

Some molecules emit fluorescence naturally while others can be modified to yield fluorescent compounds. The fluorescent compounds exhibit two characteristic spectra: an excitation spectrum and an emission spectrum. Don't have two compounds that have the same spectrum which makes fluorometry a highly specific analytical technique (So & Dong, 2002).
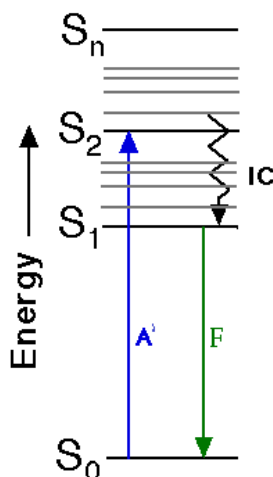
Figure 5.2 – Jablonski diagram.

where S_0, S_1, S_2 are the singlet ground, first and second electronic states, respectively; A', the photon absorption; F, the fluorescence (emission) and IC, the internal conversion.

The fluorescence measurement technique is designated fluorometry and the instrument used is called a fluorometer or fluorimeter. Fluorometry is a type of electromagnetic spectroscopy, which analyzes fluorescence from a sample and characterizes the relationship between absorbed and emitted photons at specified wavelengths. A fluorimeter generates the wavelength of light needed to excite the electrons in molecules of the sample; selectively transmitting the wavelength of the emitted light (not necessarily visible light), and then measures the intensity of the emitted light. Up to a maximum concentration, the emitted light is proportional to the concentration of the sample measured. Normally, the amount of fluorescence energy emitted is only 3% of the amount of excitation light energy. Fluorescence light has a lower energy (higher wavelength) than the excitation energy and is usually scattered light (Lakowicz, 1988) (So & Dong, 2002).

The fluorometry has several advantages such as high sensitivity and specificity, simplicity and low cost, so it is widely used for a variety of applications. This technique is about 1000 times more sensitive than absorbance measurements becoming an asset to quantitative and qualitative analysis.

5.1.3.1 – Thioflavin T Binding Assay

Thioflavin T (ThT) is a cationic benzothiazole, a classic amyloid dye that is commonly used to probe Aß fibril formation because of its strong fluorescence emission upon binding to amyloid fibril structures (Khurana, et al., 2005) (Kuznetsova, et al., 2012) (Nilsson, 2004). ThT is used to identify and quantify of amyloid fibrils as well as for the exploration of fibrillization kinetics of Aß in the presence of small molecules. It is presumed that the quantity the amyloid fibrils is proportional to the intensity of fluorescence (Biancalana & Koide, 2010) (Jameson, et al., 2012).

For ThT assays, a ThT stock solution was prepared by adding 8 mg of ThT (Sigma-Aldrich, Germany) to 10 ml of PBS (Nilsson, 2004). This solution was filtered through a 0.2 µm syringe filter and diluted (9 ml of ThT stock solution in 50 ml of PBS) (ThT working solution). To prepare specimens for kinetic studies, Aß peptide (25 µM) was incubated in the presence or ab-

sence of RES, grape seed extract and grape skin extract at the same concentrations (40 and 80 µM) in PBS, for 10 days at 37˚C. Aß peptide (25 µM) was also incubated in the presence or absence of RES-, grape seed extract- and grape skin extract-loaded PLGA NPs at the same concentrations (40 µM) in PBS, for 10 days at 37˚C. For the kinetic studies of the Aß peptides in the absence and presence of the RES and extracts of the grape seed and grape skin free and loaded in PLGA NPs, 72 µl of the samples were added to 8 µl of the ThT working solution. The samples were placed on a 96-well plate (Nunclon Delta Surface) and the fluorescence intensity was measured using a BioTek® Synergy 2 Multi-Mode reader (Winooski, Vermont, USA) after stirring 30 seconds at 37 ˚C every 20 minutes during 10 days. The spectra were subtracted to the controls (ThT working solution, drugs and PLGA NPs). The measurements were performed with a 420/50 nm excitation filter and a 485/20 nm emission filter.

5.1.4 – Transmission Electron Microscopy

Transmission electron microscopy (TEM) is used to detect the presence of fibrils. To prepare specimens for TEM imaging, Aß peptide (25 µM) was incubated in the presence or absence of RES, grape seed extract and grape skin extract free and loaded in PLGA NPs at the same concentrations (40 and 80 µM for free drugs and 40 µM for drugs-loaded PLGA NPs) in PBS, for 7 days at 37°C. For the ultra-structural studies of the Aß peptides in the absence and presence of the RES and extracts of the grape seed and grape skin free and loaded in PLGA NPs, 5 µL of each sample was placed on carbon-formvar coated 200-400 mesh spacing grids (Agar Scientific, UK) and let to adsorb for 5 minutes. The negative staining was performed with 2% (w/v) filtered aqueous solution of uranyl acetate for 45 seconds. The uranyl acetate solution was centrifuged at 12000 rpm for 3 minutes to pellet any unsolubilized uranyl acetate before use. After removing the excess of the negative staining solution and drying the grids, the samples were visualized using a Jeol JEM 1400 (Tokyo, Japan) electron microscope at 80 kV.

5.2 – Results and Discussion

5.2.1 – Interaction of Aβ with Resveratrol and Extracts of Grape Seed and Skin

Initially, the aggregation of Aß$_{(1-42)}$ was studied in the absence and presence of RES and extracts of the grape seed and grape skin at a peptide concentration of 25 µM and RES, grape seed extract and grape skin extract at two different concentrations (40 and 80 µM) in PBS, for 10 days at 37 ˚C. To evaluate the inhibitory activities of RES, extract of the grape seed and extract of the grape skin, against Aß$_{(1-42)}$ aggregation, ThT fluorescence binding assay and TEM were performed.

ThT binding assay results (Figure 5.3 and Figure 5.4) demonstrated that a significant binding to ThT is observed for Aß$_{(1-42)}$ incubated alone. The fluorescence intensity at 450 nm, which is the characteristic excitation maximum observed upon ThT binding, increased after 6 hours incubation time at 37 ˚C. The results indicated that the intensity of fluorescence of RES, extract of the grape seed and extract of the grape skin was low. These results reveal that RES and the extracts of the grape seed and skin inhibit the Aß$_{(1-42)}$ fibril formation. The results indicated that the extracts have a more pronounced inhibitory effect in comparison with RES.

All samples reached a stable signal after approximately 10 hours incubation. At the concentration of 40 µM, RES inhibits around 86% of the aggregation of the peptide, the grape skin extract inhibits around 92% and the grape seed extract inhibits around 97%. At the concentration of 80 µM, these values increased 91, 97 and 98%, respectively. As the figures 5.3 and 5.4 show, no significant changes of percentage of the peptide aggregation (P>0.05) were observed for the both concentrations used. These results suggest that beyond to contain RES that inhibits the aggregation of $A\beta_{(1-42)}$, the extracts have other polyphenols that make this inhibitory effect most pronounced.

The results in Figure 5.5 were consistent with the ThT binding assay. TEM images demonstrated that in the absence of RES or extracts $A\beta_{(1-42)}$ showed fibril formation whereas in the presence of RES or extracts, the samples appeared to be devoid of those structures. When $A\beta_{(1-42)}$ was co-incubated with RES and extracts, the number of fibrils decreased, there were numerous oligomers present in the samples but only small aggregates are observed, indicating the inhibit the $A\beta_{(1-42)}$ fibrillogenesis.

Marambaud, et al. tried to determine if RES causes the decrease of Aß levels. To this end, they treated APP695-transfected HEK293 cells with increasing concentrations of RES and analyzed Aß levels by ELISA and Western Blot (WB). Total secreted Aß, including $A\beta_{(1-40)}$ and $A\beta_{(1-42)}$, were markedly reduced by 20 – 40 µM RES after 24 hours of incubation. To determine whether the effect of RES is time-dependent, APP695-HEK293 cells were treated for different periods of time. RES did not affect Aß levels after 12 hours of incubation. The same results related to the incubation time were achieved by ThT fluorescence essay as showed in figures 5.3 and 5.4. Their data showed that RES strongly reduces Aß produced by different cell lines expressing wild type or Swedish mutant APP695 (Marambaud, et al., 2005).

Hung, et al. studied the $A\beta_{(1-40)}$ aggregation in the presence and absence of RES using ThT and TEM. The concentration of $A\beta_{(1-40)}$ and RES used was 50 µM. In the presence of RES, the fluorescence intensity was greatly attenuated. Both samples ($A\beta_{(1-40)}$ alone and $A\beta_{(1-40)}$ with RES) reached a stable signal after 144 hours. Structural modification of $A\beta_{(1-40)}$ by RES was also imaged using TEM with samples incubated for 7 days at 37˚C. Fibril networks of $A\beta_{(1-40)}$ have been observed in the absence of RES. In the presence of RES, the samples appeared to be devoid of those structures (Hung, et al., 2013). The TEM images obtained in Hung, et al. study were similar with Figure 5.5 wherein after incubation of $A\beta_{(1-42)}$ with RES also revealed a decrease of number of fibrils.

To study the effects of different concentrations of RES in inhibition of the formation of $A\beta_{(1-42)}$ aggregates, Feng, et al. mixed $A\beta_{(1-42)}$ with RES and monitored $A\beta_{(1-42)}$ aggregation using ThT. When $A\beta_{(1-42)}$ at a concentration of 10 µM was co-incubated with 2, 10, and 100 µM of RES, the level of fluorescence decreased in a concentration-dependent way, where 100 µM of RES inhibited around 90% of aggregation, 2 and 10 µM of RES inhibited 30% and 50% of fluorescence intensity, respectively, after 14 hours of incubation at 37 ˚C. The percentage of inhibition of aggregation obtained in this study at 100 µM of RES was similar to that obtained in this study using RES at 80 µM. In order to detect the morphologies of $A\beta_{(1-42)}$ aggregates, the same authors used TEM to probe the aggregation process in the presence or absence of RES. When $A\beta_{(1-42)}$ was incubated alone for 3 days, robust fibrils were observed. However when $A\beta_{(1-42)}$ was co-incubated with 10 µM and 100 µM of RES for 3 days, the number of fibrils decreased with increasing concentration of RES. At 100 µM, were observed numerous oligomers present in the samples but few fibrils were observed. TEM imaging was consistent with above fluores-

cence results (Feng, et al., 2009). Similar TEM analysis was observed as illustrated in Figure 5.4 using RES at 80 µM.

Figure 5.3 –Effect of the RES and extracts of the grape seed and grape skin on $A\beta_{(1-42)}$ fibrils content as monitored by ThT fluorescence. The $A\beta_{(1-42)}$ concentration was 25 µM and the drugs concentration was 40 µM. The samples were incubated at 37°C for 10 days in the presence or absence of RES and extracts of the grape seed and grape skin in PBS buffer.
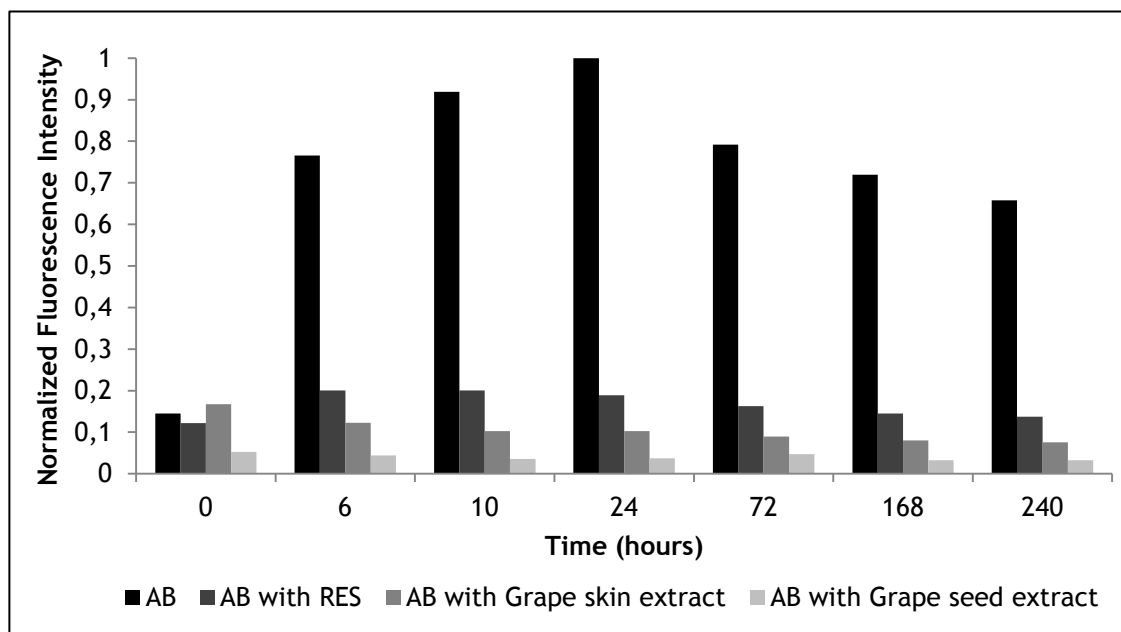

Figure 5.4 – Effect of the RES and extracts of the grape seed and grape skin on $A\beta_{(1-42)}$ fibrils content as monitored by ThT fluorescence. The $A\beta_{(1-42)}$ concentration was 25 µM and the drugs concentration was 80 µM. The samples were incubated at 37°C for 10 days in the presence or absence of RES and extracts of the grape seed and grape skin in PBS buffer.
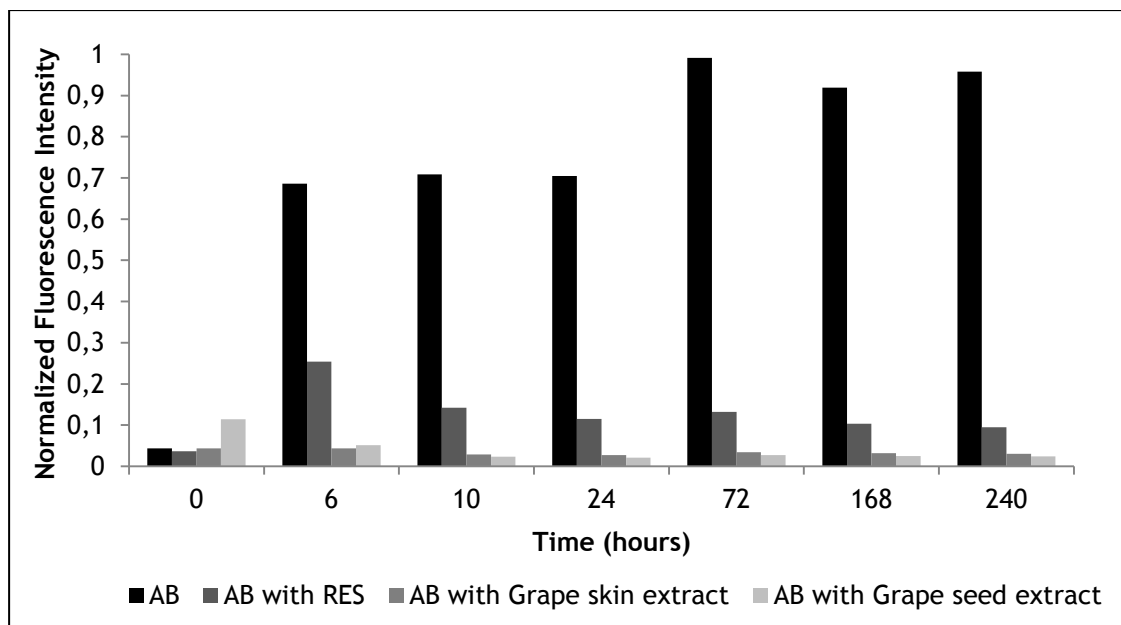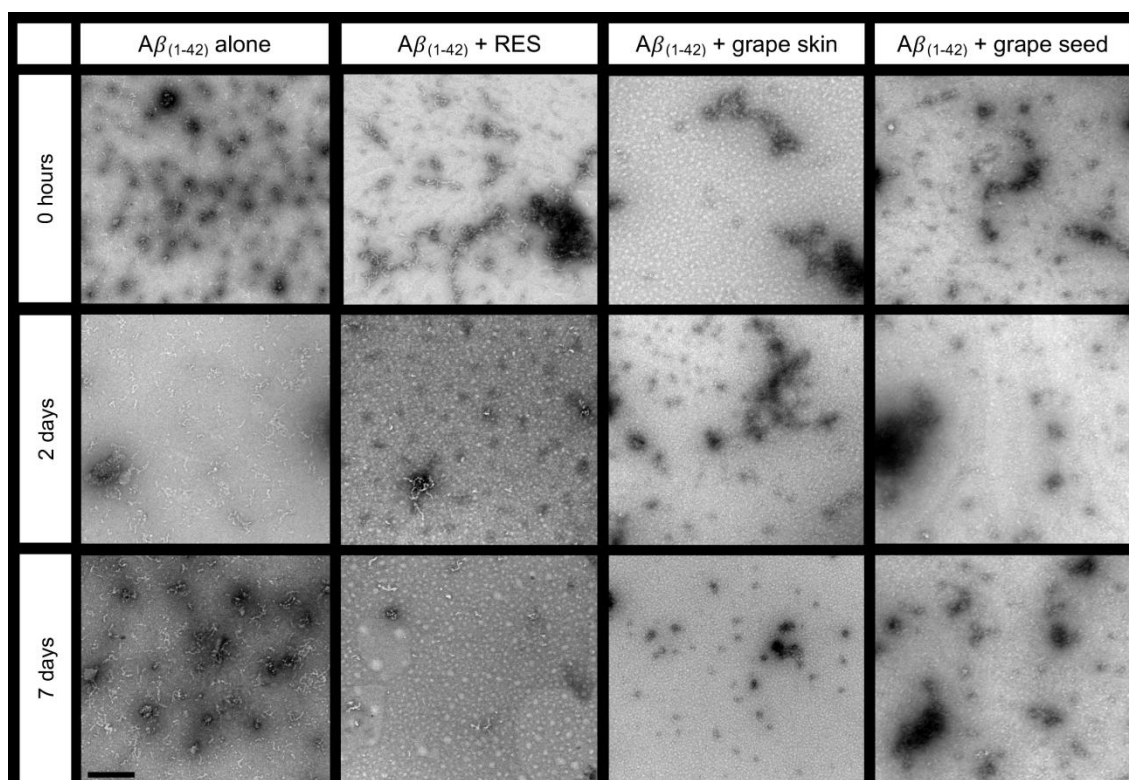
	Aβ(1-42) alone	Aβ(1-42) + RES	Aβ(1-42) + grape skin	Aβ(1-42) + grape seed
0 hours				
2 days				
7 days				

Figure 5.5 – Transmission electron microscopy of the effect of the RES and extracts of the grape seed and grape skin on Aβ(1-42) aggregation. The Aβ(1-42) concentration was 25 μM and the drugs concentration was 80 μM. The samples were incubated for 10 days at 37 °C in the presence or absence of RES and extracts of the grape seed and grape skin in PBS buffer. The scale bar corresponds to 100 nm.

Considering the results obtained, this natural compound could be a promising molecule for the development of therapeutics for prevent or treat AD.

The aggregation of Aβ(1-42) was also studied in the presence of loaded-PLGA NPs at a peptide concentration of 25 μM and drugs concentrations of 40 μM in PBS, for 10 days at 37 °C. To evaluate the inhibitory activities of loaded-PLGA NPs against Aβ(1-42) aggregation, ThT fluorescence binding assay and TEM were performed.

ThT binding assay results (Figure 5.6) demonstrated that a significant binding to ThT is observed for Aβ(1-42) incubated alone. The fluorescence intensity at 450 nm, which is the characteristic excitation maximum observed upon ThT binding, increased after 6 hours incubation time at 37 °C. The results indicated that the intensity of fluorescence of Aβ(1-42) with drug-loaded PLGA NPs was lower in comparison with Aβ(1-42) alone. These results reveal that drug-loaded PLGA NPs inhibit the Aβ(1-42) fibril formation. The results indicated that the extracts-loaded PLGA NPs have a more pronounced inhibitory effect in comparison with RES-loaded PLGA NPs. After approximately 6 hours incubation, all samples showed a slow decrease of normalized fluorescence intensity. At the concentration of 40 μM, RES-loaded PLGA NPs inhibits around 46% of the aggregation of the peptide, the grape skin extract-loaded PLGA NPs inhibits around 52% and the grape seed extract-loaded PLGA NPs inhibits around 56%, after 10 days of incubation.

The results in Figure 5.7 were consistent with the ThT binding assay. TEM images demonstrated that in the absence of RES or extracts Aβ(1-42) showed fibril formation. In the presence of RES or extracts, the samples in the presence of the drug, the quantity of fibers present in

the samples appears to be lower with the observation oligomers and protofibrils, indicating the inhibit the Aβ$_{(1-42)}$ fibrillogenesis.
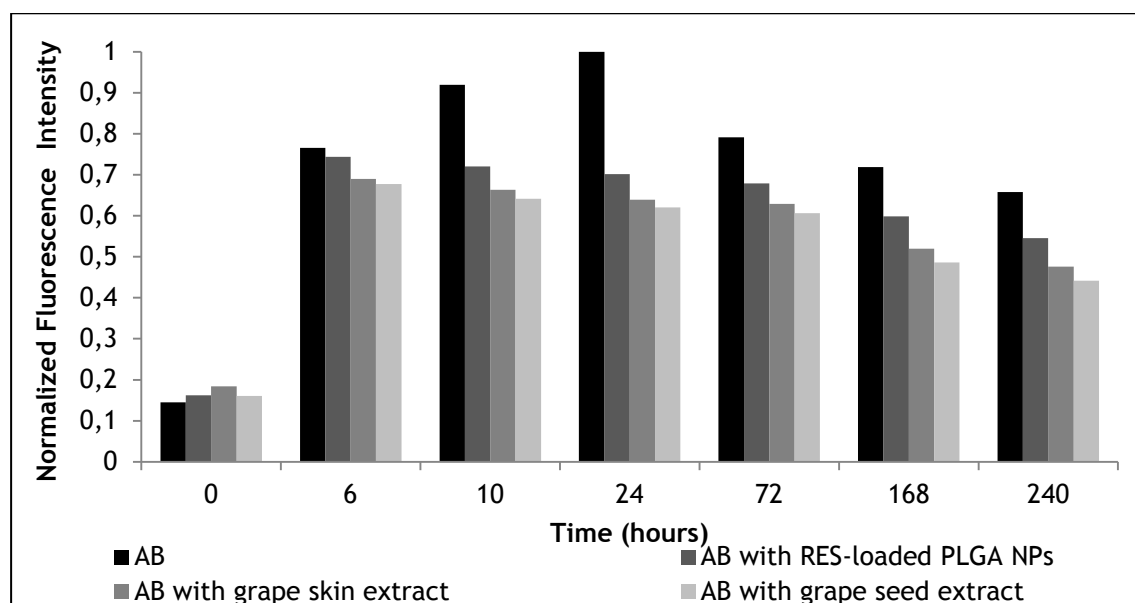
Figure 5.6 – Effect of loaded-PLGA NPs on Aβ$_{(1-42)}$ fibrils content as monitored by ThT fluorescence. The Aβ$_{(1-42)}$ concentration was 25 μM and the drugs concentration was 40 μM. The samples were incubated at 37˚C for 10 days in the presence or absence of loaded-PLGA NPs in PBS buffer.
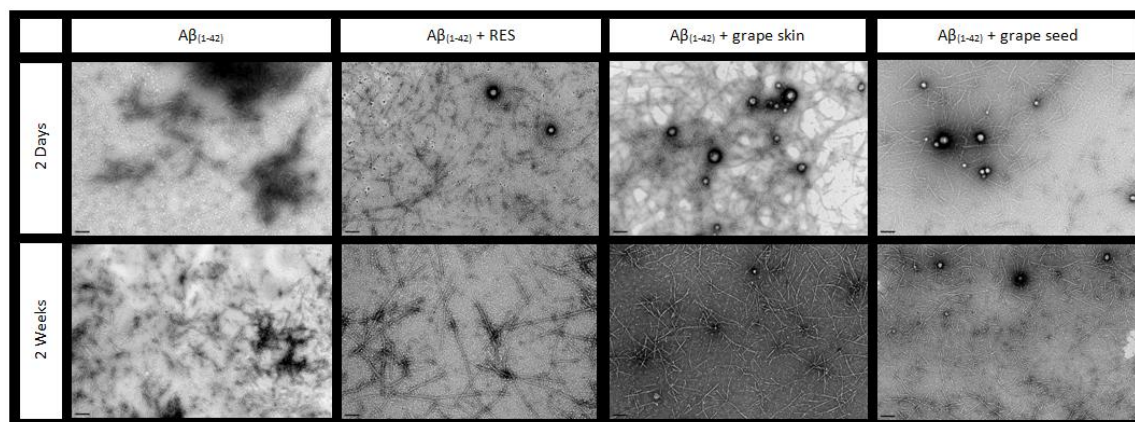
Figure 5.7 – Transmission electron microscopy of the effect of the loaded-PLGA NPs on Aβ$_{(1-42)}$ aggregation. The Aβ$_{(1-42)}$ concentration was 25 μM and the drugs concentration was 40 μM. The samples were incubated for 14 days at 37 ˚C in the presence or absence of loaded-PLGA NPs in PBS buffer. The scale bar corresponds to 200 nm.

Chapter 6

Concluding Remarks and Future Perspectives

The AD, a neurodegenerative disorder, is promoted by the increase of the age. This disease is a progressive disease and is characterized by loss of memory and cognitive impairment, loss of language and behavior changes. The neuropathological characteristics of AD include extracellular senile plaques, which consist of deposits of Aß and neurofibrillar tangles that are formed by hyperphosphorilation and abnormal deposition of tau protein (Clippingdale, et al., 2001) (Klafki, et al., 2006) (Selkoe, 2001). The imbalance between Aß production and its clearance leads to the Aß aggregation in the brain, that plays a key role in the development of AD (Li, et al., 2012).

Insoluble fibrillar protein aggregates are considered a pathological feature of AD. Protein misfolding or partially folded structure is responsible for the fibrillation of various amyloidogenic proteins/peptides (Ahn, et al., 2007). Thus, it is essential to find molecules that prevent or interrupt the aggregation of proteins (Feng, et al., 2009).

RES arouses great interest because has interesting biochemical and physiological properties (Ahn, et al., 2007) (Amri, et al., 2012) (Baur & Sinclair, 2006). Several studies have demonstrated that RES is capable of preventing a variety of disorders, including cardiovascular diseases, cancer, diabetes, arthritis and neurodegenerative diseases. Given the benefits of RES, it is believed that it is useful in the therapy of AD and PD (Gusman, et al., 2001). RES has anti-amyloidogenic activity because it promotes the intracellular degradation of Aß by a mechanism involving the proteasome, thereby reducing levels of Aß (Marambaud, et al., 2005).

A growing effort has being applied to find novel approaches for neurodegenerative treatment and in recent years a growing number of studies, focused on the research and development of NPs as drug delivery systems, have been conducted (Wilczewska, et al., 2012). Nanoparticles are promising candidates for drugs delivery, as they present numerous advantages over conventional chemotherapy such as improving the drug water solubility, protecting it

from the macrophage uptake, thus enhancing the blood circulation time, and finally providing an increased and controlled release into the specific final target.

Liposomes and PLGA have different physico chemical, biochemical and mechanical properties each presenting their own advantages where drug delivery is concerned. For this reason, in this work, liposomes and PLGA NPs were proposed to drug delivery to AD.

Drug-loaded liposomes were not able to encapsulate RES and extracts, no significant values of encapsulation efficiency were obtained for these nanocarriers.

Drug-loaded PLGA NPs were prepared by a single emulsion solvent evaporation method and stabilized with Pluronic® F-127. Two experimental conditions were tested and discussed using RES and extracts of grape seed and skin as a drug model to select the NP that presents adequate physicochemical characteristics for the drugs encapsulation and delivery. The prepared PLGA NPs exhibit a spherical shape, mean diameter ranging between 158 to 182 nm, low PdI values and negative zeta potential values. While RES entrapment reached values of efficiency of approximately 80±6 %, for grape seed and skin extracts-loaded PLGA NPs the attained encapsulation efficiency values were slightly lower, 75±5 % and 74±8 %, respectively. The prepared NPs exhibited loading capacity values in the order of 0.3-7 % and a process yield in the order of 3.4-6.6 %. The prepared system is stable at storage conditions for one month.

ThT binding assay and TEM results demonstrated that RES, extract of the grape seed and extract of the grape skin inhibit the $A\beta_{(1-42)}$ fibril formation. The results indicated that the extracts have a more pronounced inhibitory effect in comparison with RES. At the concentration of 40 µM, RES inhibits around 86% of the aggregation of the peptide, the grape skin extract inhibits around 92% and the grape seed extract inhibits around 97%. At the concentration of 80 µM, these values increased for 91, 97 and 98%, respectively. No significant changes of percentage of the peptide aggregation (P>0.05) were observed for the both concentrations used. These results suggest that beyond to contain RES that inhibits the aggregation of $A\beta_{(1-42)}$, the extracts have other polyphenols that make this inhibitory effect most pronounced.

The studies proved that drug-loaded PLGA NPs inhibit the $A\beta_{(1-42)}$ fibril formation. The results indicated that the extracts-loaded PLGA NPs have a more pronounced inhibitory effect in comparison with RES-loaded PLGA NPs. At the concentration of 40 µM, RES-loaded PLGA NPs inhibits around 46% of the aggregation of the peptide, the grape skin extract-loaded PLGA NPs inhibits around 52% and the grape seed extract-loaded PLGA NPs inhibits around 56%, after 10 days of incubation.

All these results suggest that the obtained NPs could be good candidates for RES and extracts of grape seed and skin release. The nanoencapsulation in PLGA NPs may offer a new and potentially effective administration strategy of RES and extracts of grape seed and skin that overcomes the actual limitations as its bioavailability and toxicity. But, the optimization of NPs must be performed.

Several assays and experiments could have been conducted to upgrade the developed system as to improve its characterization, but were not possible to perform due to time restrictions. Although, the prepared PLGA NPs have proved to be a promising new approach to RES and extracts of grape seed and skin delivery to AD, further development is required. The optimization of NPs must be performed in order to increase the therapeutic potential of the drugs under study. For instance surface modification, with specific biomolecules or antibodies, may improve their targeting and accumulation in target-tissue as increase their bioavailability. Finally, in vivo tests using animal models would be interesting to evaluate in detail the system efficacy. However these studies would entail a costly investment.

Appendix

$y = 0{,}0143x$
$R^2 = 0{,}995$
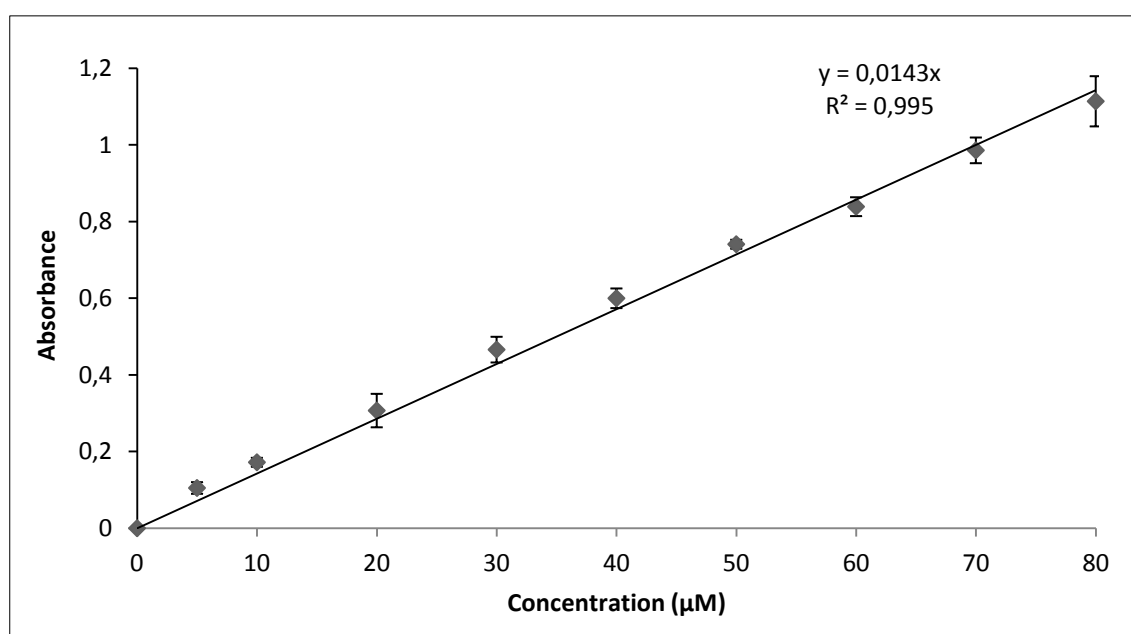
Appendix 1 - Calibration curve of RES using BioTek® Synergy 2 Multi-Mode Reader (n=3).

The plot shows a calibration curve with the equation $y = 0{,}0363x$ and $R^2 = 0{,}9989$. The y-axis is labeled "Absorbance" ranging from 0 to 1,6. The x-axis is labeled "Concentration (µM)" ranging from 0 to 40.
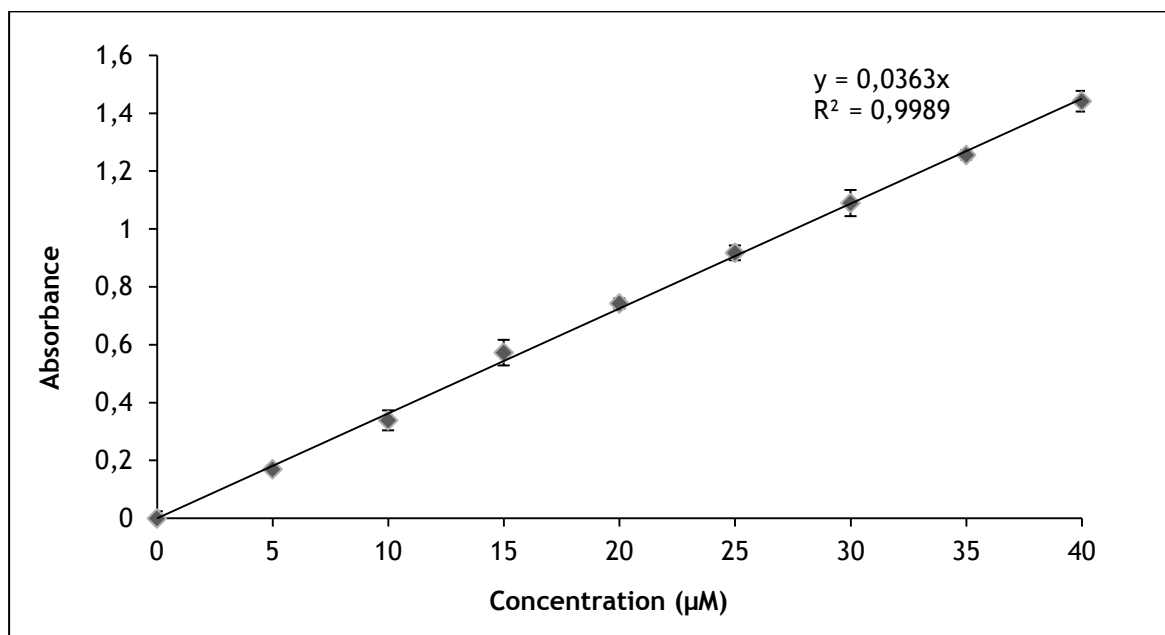
Appendix 2 - Calibration curve of RES using UV-1700 PharmaSpec UV-VIS Spectrophotometer Shimadzu (n=3).

References

Royal Society of Chemistry- Advancing the Chemical Sciences, 2009. Introduction to Ultraviolet - Visible Spectroscopy. In: *Ultraviolet - Visible Spectroscopy (UV)*. s.l.:s.n.

Abbott, J., 2004. Evidence for bulk flow of brain interstitial fluid: significance for physiology and pathology. *Neurochemistry International,* Volume 45, p. 545–552.

Abbott, J. et al., 2010. Structure and function of the blood–brain barrier. *Neurobiology of Disease,* Volume 37, p. 13–25.

Abbott, J., Rönnbäck, L. & Hansson, E., 2006. Astrocyte–endothelial interactions at the blood–brain barrier. *Neuroscience,* Volume 7, pp. 41-53.

Acharya, S. & Sahoo, S. K., 2011. PLGA nanoparticles containing various anticancer agents and tumour delivery by EPR effect. *Advanced Drug Delivery Reviews,* Volume 63, p. 170–183.

Ahmed, M. et al., 2010. Structural conversion of neurotoxic amyloid-ß1–42 oligomers to fibrils. *Nature structural & molecular biology,* Volume 5, pp. 561-567.

Ahn, J., Lee, J.-H., Kim, J.-H. & Paik, S., 2007. Novel method for quantitative determination of amyloid fibrils of alpha-synuclein and amyloid beta/A4 protein by using resveratrol. *Analytical Biochemistry,* Volume 367, p. 259-265.

Akbarzadeh, A. et al., 2013. Liposome: classification, preparation, and applications. *Nanoscale Research Letters,* Volume 8, pp. 1-9.

Alam, I. et al., 2010. Strategy for effective brain drug delivery. *European Journal of Pharmaceutical Sciences,* Volume 40, p. 385–403.

Albani, D. et al., 2009. The SIRT1 activator resveratrol protects SK-N-BE cells from oxidative stress and against toxicity caused by alpha-synuclein or amyloid-beta (1-42) peptide. *Journal of Neurochemistry,* Volume 110, p. 1445-1456.

Albani, D., Polito, L., Signorini, A. & Forloni, G., 2010. Neuroprotective properties of resveratrol in different neurodegenerative disorders. *International Union of Biochemistry and Molecular Biology,* Volume 36, p. 370-376.

Alves, L. et al., 2012. Alzheimer's disease: a clinical practice-oriented review. *Frontiers in Neurology,* Volume 3, pp. 1-20.

Amri, A., Chaumeil, C., Sfar, S. & Charrueau, C., 2012. Administration of resveratrol: What formulation solutions to bioavailability limitations?. *Journal of Controlled Release,* pp. 182-193.

Anekonda, T., 2006. Resveratrol—A boon for treating Alzheimer's disease?. *Brain Research Reviews,* Volume 52, pp. 316-326.

Anekonda, T. & Reddy, H., 2005. Can herbs provide a new generation of drugs for treating Alzheimer's disease?. *Brain Research Reviews,* Volume 50, p. 361 – 376.

Anwekar, H., Patel, S. & Singhai, A., 2011. Liposome - as drug carriers. *International Journal of Pharmacy & Life Sciences,* pp. 945-951.

Armstrong, R., 2011. The Pathogenesis of Alzheimer's Disease: A Reevaluation of the "Amyloid Cascade Hypothesis". *International Journal of Alzheimer's Disease,* pp. 1-6.

Asadabad, M. A. & Eskandari, M. J., 2015. Transmission Electron Microscopy as Best Technique for Characterization in Nanotechnology. *Synthesis and Reactivity in Inorganic, Metal-Organic, and Nano-Metal Chemistry,* Volume 15, p. 323–326.

Bartels, T., Choi, J. & Selkoe, D., 2011. Alpha-Synuclein occurs physiologically as a helically folded tetramer that resists aggregation. *Nature,* Volume 477, pp. 107-111.

Baur, J. & Sinclair, D., 2006. Therapeutic potential of resveratrol: the in vivo evidence. *Nature reviews Drug discovery,* pp. 493-506.

Beal, F., 2003. Mitochondria, oxidative damage, and inflammation in Parkinson's disease. *New York Academy of Science,* Volume 991, p. 120–131.

Bernacki, J., Dobrowolska, A., Nierwiñska, K. & Malecki, A., 2008. Physiology and pharmacological role of the blood-brain barrier. *Pharmacological Reports,* Volume 60, p. 600–622.

Berne, B. & Pecora, R., 1976. *Dynamic Light Scattering: With Applications to Chemistry, Biology, and Physics.* New York: s.n.

Biancalana, M. & Koide, S., 2010. Molecular Mechanism of Thioflavin-T Binding to Amyloid Fibrils. *Biochim Biophys Acta,* Volume 7, pp. 1-17.

Blennow, K., de Leon, M. & Zetterberg, H., 2006. Alzheimer's disease. *The Lancet,* Volume 368, p. 387–403.

Boado, R. & Pardridge, W., 2011. The Trojan Horse Liposome Technology for Nonviral Gene Transfer across the Blood-Brain Barrier. *Journal of Drug Delivery,* pp. 1-12.

Boado, R., Zhang, Y., Zhang, Y. & Pardridge, W., 2007. Humanization of Anti-Human Insulin Receptor Antibody for Drug Targeting Across the Human Blood–Brain Barrier. *Biotechnology and Bioengineering,* Volume 96, pp. 381-291.

Boer, A. & Gaillard, P., 2007. Drug Targeting to the Brain. *Annual Review of Pharmacology and Toxicology,* Volume 47, p. 323–55.

Bonechi, C. et al., 2012. Using Liposomes as Carriers for Polyphenolic Compounds: The Case of Trans-Resveratrol. *PLOS ONE,* Volume 8, pp. 1-11.

Boyd, R. D., Pichaimuthu, S. K. & Cuenat, A., 2011. New approach to inter-technique comparisons for nanoparticle size measurements; using atomic force microscopy, nanoparticle tracking analysis and dynamic light scattering. *Colloids and Surfaces A: Physicochemical and Engineering Aspects,* Volume 387, pp. 35-42.

Brigger, I., Dubernet, C. & Couvreur, P., 2002. Nanoparticles in cancer therapy and diagnosis. *Advanced Drug Delivery Reviews,* Volume 54, p. 631–651.

Brookmeyer, R., Johnson, E., Ziegler-Graham, K. & Arrighi, H., 2007. Forecasting the global burden of Alzheimer's disease. *Alzheimer's & Dementia,* Volume 3, p. 186–191.

Caddeo, C. et al., 2013. Nanocarriers for antioxidant resveratrol: Formulation approach, vesicle self-assembly and stability evaluation. *Colloids and Surfaces B: Biointerfaces,* Volume 111, p. 327– 332.

Cahn, R. W. & Haasen, P., 1996. *Physical metallurgy.* 4th ed. Amsterdão; New York: North-Holland: rev. and enhanced.

Candela, P. et al., 2010. Apical-to-Basolateral Transport of Amyloid-beta Peptides through Blood-Brain Barrier Cells is Mediated by the Receptor for Advanced Glycation End-Products and is Restricted by P-Glycoprotein. *Journal of Alzheimer's Disease,* Volume 22, p. 849-859.

Cao, S., Wang, D., Tan, X. & Chen, J., 2009. Interaction Between Trans-resveratrol and Serum Albumin in Aqueous Solution. *Journal of Solution Chemistry ,* Volume 38, p. 1193-1202.

Cassiano, N. M. et al., 2009. Validação em métodos cromatográficos para análises de pequenas moléculas em matrizes biológicas. *Química Nova,* pp. 1021-1030.

Chachay, V. et al., 2011. Resveratrol – pills to replace a healthy diet?. *British Journal of Clinical,* pp. 27-38.

Chen, J. et al., 2005. SIRT1 Protects against Microglia-dependent Amyloid- β Toxicity through Inhibiting NF- κB Signaling. *The Journal of Biological Chemistry,* Volume 280, p. 40364 –40374.

Choi, W.-S., Palmiter, R. & Xia, Z., 2011. Loss of mitochondrial complex I activity potentiates dopamine neuron death induced by microtubule dysfunction in a Parkinson's disease model. *The Journal of Cell Biology,* Volume 192, p. 873–882.

Clippingdale, A., Wade, J. & Barrow, C., 2001. The beta-Amyloid Peptide and its Role in Alzheimer's Disease. *Journal of Peptide Science,* Volume 7, p. 227-249.

Cohen, S. et al., 1991. Controlled delivery systems for proteins based on poly(lactic/glycolic acid) microspheres. *Pharmaceutical Research,* Volume 8, pp. 713-20.

Conte, A., Pellegrini, S. & Tagliazucchi, D., 2003. Synergistic protection of PC12 cells from beta-amyloid toxicity by resveratrol and catechin. *Brain Research Bulletin,* Volume 62, pp. 29-38.

Crone, C. & Christensen, O., 1981. Electrical Resistance of a Capillary Endothelium. *The Journal of General Physiology,* Volume 77, pp. 349-371.

Danhier, F. et al., 2012. PLGA-based nanoparticles: An overview of biomedical applications. *Journal of Controlled Release,* Volume 161, p. 505–522.

Defazio, G., Gigante, A., Mancino, P. & Tinazzi, M., 2013. The epidemiology of pain in Parkinson's disease. *Journal of Neural Transmission ,* p. 583–586.

Delmas, D. et al., 2001. Transport, stability, and biological activity of resveratrol. *Annals of the New York academy of sciences,* p. 48–59.

Devine, M., Gwinn, K., Singleton, A. & Hardy, J., 2011. Parkinson's Disease and alpha-Synuclein Expression. *Movement Disorders,* Volume 26, pp. 2160-2168.

Dua, J. S., Rana, A. C. C. & Bhandari, A. K., 2012. Liposome: Methods of Preparation and Applications. *International Journal of Pharmaceutical Studies and Research,* Volume 3, pp. 14-20.

El-Kabbany, F., Taha, S. & Hafez, M., 2014. A study of the phase transition of reheated diphenyl carbazide (DPC) by using UV spectroscopy. *Spectrochimica Acta Part A: Molecular and Biomolecular Spectroscopy,* Volume 128, p. 481–488.

Emborg, M., 2004. Evaluation of animal models of Parkinson's disease for neuroprotective strategies. *Journal of Neuroscience Methods,* Volume 139, p. 121–143.

Engelhart, M. et al., 2002. Dietary Intake of Antioxidants and Risk of Alzheimer Disease. *Journal of the American Medical Association,* Volume 287, pp. 3223-3229.

Feng, Y. et al., 2009. Resveratrol inhibits beta-amyloid oligomeric cytotoxicity but does not prevent oligomer formation. *NeuroToxicology,* Volume 30, p. 986–995.

Ferretta, A. et al., 2014. Effect of resveratrol on mitochondrial function: Implications in parkin-associated familiar Parkinson's disease. *Biochimica et Biophysica Acta,* Volume 1842, p. 902-915.

Ferri, C. et al., 2005. Global prevalence of dementia: a Delphi consensus study. *The Lancet,* Volume 366, p. 2112–2117.

Fessi, H., Puisieux, J. P., Ammoury, N. & Benita, S., 1989. Nanocapsule formation by interfacial polymer deposition following solvent displacement. *International Journal of Pharmaceutics,* Volume 55, pp. R1-R4.

Filip, V. et al., 2013. Resveratrol and its antioxidant and antimicrobial effectiveness. *Food Chemistry,* p. 585–593.

Frasco, M. F. et al., 2014. Transferrin surface-modified PLGA nanoparticles-mediated delivery of a proteasome inhibitor to human pancreatic cancer cells. *Journal of Biomedical Materials Researsh A,* pp. 1-9.

Friedman, L. et al., 2012. Disrupted Autophagy Leads to Dopaminergic Axon and Dendrite Degeneration and Promotes Presynaptic Accumulation of alpha-Synuclein and LRRK2 in the Brain. *The Journal of Neuroscience,* Volume 32, p. 7585–7593.

Frye, R., 2000. Phylogenetic Classification of Prokaryotic and Eukaryotic Sir2-like Proteins. *Biochemical and Biophysical Research Communications,* Volume 273, p. 793–798.

Gabizon, A., Shmeeda, H. & Barenholz, Y., 2003. Pharmacokinetics of Pegylated Liposomal Doxorubicin. *Clinical Pharmacokinetics,* Volume 42, pp. 419-436.

Gaggelli, E., Kozlowsk, H., Valensin, D. & Valensin, G., 2006. Copper Homeostasis and Neurodegenerative Disorders (Alzheimer's, Prion, and Parkinson's Diseases and Amyotrophic Lateral Sclerosis). *Chemical Reviews,* p. 1995–2044.

Gao, D. et al., 2006. Resveratrol reduces the elevated level of MMP-9 induced by cerebral ischemia–reperfusion in mice. *Life Sciences,* Volume 78, p. 2564 – 2570.

Giovinazzo, G. et al., 2012. Resveratrol Biosynthesis: Plant Metabolic Engineering for Nutritional Improvement of Food. *Plant Foods for Human Nutrition,* p. 191–199.

Goetz, C., 2014. The History of Parkinson's Disease: Early Clinical Descriptions and Neurological Therapies. *Cold Spring Harbor Perspectives in Medicine,* pp. 1-15.

Gonçalves, C. et al., 2014. Lipopolyplexes comprising imidazole/imidazolium lipophosphoramidate, histidinylated polyethyleneimine and siRNA as efficient formulation for siRNA transfection. *International Journal of Pharmaceutics,* Volume 460, pp. 264-272.

Gralle, M. & Ferreira, S., 2007. Structure and functions of the human amyloid precursor protein: The whole is more than the sum of its parts. *Progress in Neurobiology,* Volume 82, p. 11–32.

Greenamyre, T., Sherer, T., Betarbet, R. & Panov, A., 2001. Complex I and Parkinson's Disease. *International Union of Biochemistry and Molecular Biology Life,* Volume 52, p. 135–141.

Gusman, J., Malonne, H. & Atassi, G., 2001. A reappraisal of the potential chemopreventive and chemotherapeutic properties of resveratrol. *Carcinogenesis,* pp. 1111-1117.

Haigis, M. & Guarente, L., 2006. Mammalian sirtuins––emerging roles in physiology, aging, and calorie restriction. *Genes & Development,* Volume 20, p. 2913–2921.

Hans, M. L. & Lowman, A. M., 2002. Biodegradable nanoparticles for drug delivery and targeting. *Current Opinion in Solid State and Materials Science,* Volume 6, p. 319–327.

Hardy, J. & Selkoe, D., 2002. The Amyloid Hypothesis of Alzheimer's Disease: Progress and Problems on the Road to Therapeutics. *Science's Compass,* Volume 297, pp. 353-356.

Hervé, F., Ghinea, N. & Scherrmann, J.-M., 2008. CNS Delivery Via Adsorptive Transcytosis. *American Association of Pharmaceutical Scientists,* Volume 10, pp. 455-472.

Hiemenz, P. C. & Rajagopalan, R., 1997. *Principles of colloid and surface chemistry.* 3rd ed. New York: Marcel Dekker: s.n.

Howes, M.-J. & Houghton, P., 2003. Plants used in Chinese and Indian traditional medicine for improvement of memory and cognitive function. *Pharmacology, Biochemistry and Behavior,* Volume 75, p. 513 – 527.

Huang, F.-Y.et al., 2013. In Vitro and in Vivo Evaluation of Lactoferrin-Conjugated Liposomes as a Novel Carrier to Improve the Brain Delivery. *International Journal of Molecular Sciences,* Volume 14, pp. 2862-2874.

Hung, V. W. S. et al., 2013. Electrochemical Detection of Amyloid-Beta Aggregation in the Presence of Resveratrol. *Journal of The Electrochemical Society,* Volume 160, pp. G3097-G3101.

Iacopini, P., Baldi, M., Storchi, P. & Sebastiani, L., 2008. Catechin, epicatechin, quercetin, rutin and resveratrol in red grape: Content, in vitro antioxidant activity and interactions. *Journal of Food Composition and Analysis,* Volume 21, p. 589– 598.

Irwin, D., Lee, V. & Trojanowski, J., 2013. Parkinson's disease dementia: convergence of α-synuclein, tau and amyloid-ß pathologies. *Neuroscience,* Volume 14, pp. 626-636.

Isailović, B. D. et al., 2013. Resveratrol loaded liposomes produced by different techniques. *Innovative Food Science and Emerging Technologies,* Volume 19, p. 181–189.

Jafari, S. M., He, Y. & Bhandari, B., 2006. Nano-Emulsion Production by Sonication and Microfluidization—A Comparison. *International Journal of Food Properties,* Volume 9, p. 475–485.

Jain, R. A., 2000. The manufacturing techniques of various drug loaded biodegradable poly(lactide-co-glycolide) (PLGA) devices. *Biomaterials,* Volume 21, pp. 2475-2490.

Jameson, P. L., Smith, N. W. & Dzyuba, S. V., 2012. Dye-Binding Assays dor Evaluation of the Effects of Small Molecule Inhibitors on Amyloid Self-Assembly. *CS Chemical Neuroscience,* Volume 3, pp. 807-819.

Jang, J.-H. & Surh, Y.-J., 2003. Protective Effect of Resveratrolon Beta-Amyloid-Induced Oxidative PC12 Cell Death. *Free Radical Biology & Medicine,* Volume 34, pp. 1100-1110.

Jang, M. et al., 2007. Resveratrol Oligomers from Vitis amurensis Attenuate beta-Amyloid-Induced Oxidative Stress in PC12 Cells. *Biological & Pharmaceutical Bulletin,* Volume 30, p. 1130—1134.

Jankovic, J., 2008. Parkinson's disease: clinical features and diagnosis. *Journal of Neurology, Neurosurgery and Psychiatry,* Volume 79, p. 368–376.

Jiang, J. & Oberdorster, G., 2009. Characterization of size, surface charge, and agglomeration state of nanoparticle dispersions for toxicological studies. *Journal of Nanoparticle Research,* Volume 11, p. 77–89.

Kalaria, R. et al., 2008. Alzheimer's disease and vascular dementia in developing countries: prevalence, management, and risk factors. *The Lancet Neurology,* Volume 7, p. 812–826.

Kalinderi, K., Fidani, L., Katsarou, Z. & Bostantjopoulou, S., 2011. Pharmacological treatment and the prospect of pharmacogenetics in Parkinson's disease. *International Journal of Clinical Practice,* Volume 65, p. 1289-1294.

Karran, E., Mercken, M. & Strooper, B., 2011. The amyloid cascade hypothesis for Alzheimer's disease: an appraisal for the development of therapeutics. *Nature Reviews Drugs Discovery,* Volume 10, pp. 698-712.

Karuppagounder, S. et al., 2009. Dietary supplementation with resveratrol reduces plaque pathology in a transgenic model of Alzheimer's disease. *Neurochemistry International,* Volume 54, p. 111–118.

Kawasaki, E. S. & Player, A., 2005. Nanotechnology, nanomedicine, and the development of new, effective therapies for cancer. *Nanomedicine,* Volume 1, pp. 101-9.

Keller, J., Hanni, K. & Markesbery, W., 2000. Impaired Proteasome Function in Alzheimer's Disease. *Journal of Neurochemistry,* Volume 62, p. 302–310.

Kentish, S. et al., 2008. The use of ultrasonics for nanoemulsion preparation. *Innovative Food Science and Emerging Technologies,* Volume 9, p. 170–175.

Khurana, R. et al., 2005. Mechanism of thioflavin T binding to amyloid fibrils. *Journal of Structural Biology,* Volume 151, pp. 229-238.

Kim, D. et al., 2007. SIRT1 deacetylase protects against neurodegeneration in models for Alzheimer's disease and amyotrophic lateral sclerosis. *The EMBO Journal,* Volume 26, p. 3169–3179.

Klafki, H., Staufenbiel, M., Kornhuber, J. & Wiltfang, J., 2006. Therapeutic approaches to Alzheimer's disease. *Brain,* Volume 129, p. 2840–2855.

Klose, D., Siepmann, F., Elkharraz, K. & Siepmann, J., 2008. PLGA-based drug delivery systems: Importance of the type of drug and device geometry. *International Journal of Pharmaceutics,* Volume 354, p. 95–103.

Korczyn, A., 2008. The amyloid cascade hypothesis. *Alzheimer's & Dementia,* Volume 4, p. 176–178.

Kristl, J. et al., 2009. Improvements of cellular stress response on resveratrol in liposomes. *European Journal of Pharmaceutics and Biopharmaceutics,* p. 253–259.

Kumari, A., Yadav, S. & Yadav, S., 2010. Biodegradable polymeric nanoparticles based drug delivery systems. *Colloids and Surfaces B: Biointerfaces,* Volume 75, pp. 1-18.

Kuznetsova, I. M., Sulatskaya, A. I., Uversky, V. N. & Turoverov, K. K., 2012. Analyzing Thioflavin T Binding to Amyloid Fibrils by an Equilibrium Microdialysis-Based Technique. *PLOS ONE,* Volume 7, pp. 1-8.

Ladiwala, A. et al., 2012. Conformational Differences between Two Amyloid-beta Oligomers of Similar Size and Dissimilar Toxicity. *The Journal of Biological Chemestry,* Volume 287, p. 24765-24773.

Lakowicz, R. J., 1988. Principles of Frequency-Domain Fluorescence Spectroscopy and Applications to Cell Membranes. *Subcellular Biochemistry,* Volume 13, pp. 89-126.

Laouini, A. et al., 2012. Preparation, Characterization and Applications of Liposomes: State of the Art. *Journal of Colloid Science and Biotechnology,* Volume 1, p. 147–168.

Larson, E. et al., 2004. Survival after Initial Diagnosis of Alzheimer Disease. *Annals of Internal Medicine,* pp. 501-509.

Lasic, D. D., 1997. *Liposomes in Gene Delivery.* USA: CRC Press.

Lau, L. & Breteler, M., 2006. Epidemiology of Parkinson's disease. *The Lancet Neurology,* Volume 5, pp. 525-535.

Lee, H.-g.et al., 2004. Perspectives on the Amyloid-β Cascade Hypothesis. *Journal of Alzheimer's Disease,* Volume 6, p. 137–145.

Liazid, A., Palma, M., Brigui, J. & Barroso, C. G., 2007. Investigation on phenolic compounds stability during microwave-assisted extraction. *Journal of Chromatography A,* Volume 1140, pp. 29-34.

Li, F., Gong, Q., Dong, H. & Shi, J., 2012. Resveratrol, A Neuroprotective Supplement for Alzheimer's Disease. *Current Pharmaceutical Design,* pp. 27-33.

Li, M., Rouaud, O. & Poncelet, D., 2008. Microencapsulation by solvent evaporation: State of the art for process engineering approaches. *International Journal of Pharmaceutics,* Volume 363, p. 26–39.

Lin, T.-K.et al., 2014. Resveratrol Partially Prevents Rotenone-Induced Neurotoxicity in Dopaminergic SH-SY5Y Cells through Induction of Heme Oxygenase-1 Dependent Autophagy. *International Journal of Molecular Sciences,* Volume 15, pp. 1625-1646.

Lin, T.-K.et al., 2009. Mitochondrial Dysfunction and Biogenesis in the Pathogenesis of Parkinson's Disease. *Chang Gung Medical Journal,* Volume 32, pp. 589-599.

Lipinski, C., 2000. Drug-like properties and the causes of poor solubility and poor permeability. *Journal of Pharmacological and Toxicological Methods,* Volume 44, pp. 235-249.

Liu, Y. et al., 2012. The shape of things to come: importance of design in nanotechnology for drug delivery. *Therapeutic delivery,* Volume 3, p. 181–194.

Li, Y., Cao, Z. & Zhu, H., 2006. Upregulation of endogenous antioxidants and phase 2 enzymes by the red wine polyphenol, resveratrol in cultured aortic smooth muscle cells leads to cytoprotection against oxidative and electrophilic stress. *Pharmacological Research,* Volume 53, pp. 6-15.

Loscher, W. & Potschka, H., 2005. Blood-Brain Barrier Active Efflux Transporters: ATP-Binding Cassette Gene Family. *The Journal of the American Society for Experimental NeuroTherapeutics,* Volume 2, p. 86 –98.

Lotharius, J. & Brundin, P., 2002. Pathogenesis of Parkinson's Disease: Dopamine, Vesicles and Alpha-Synuclein. *Neuroscience,* Volume 3, pp. 1-11.

Lu, X.-Y., Hu, S., Jin, Y. & Qiu, L.-Y., 2012. Application of liposome encapsulation technique to improve anti-carcinoma effect of resveratrol. *Drug Development and Industrial Pharmacy,* Volume 38, p. 314–322.

Makadia, H. K. & Siegel, S. J., 2011. Poly Lactic-co-Glycolic Acid (PLGA) as Biodegradable Controlled Drug Delivery Carrier. *Polymers,* Volume 13, p. 1377–1397.

Malam, Y., Loizidou, M. & Seifalian, A., 2009. Liposomes and nanoparticles:nanosized vehicles for drug delivery in cancer. *Journal of Pharmacological Sciences,* pp. 592-599.

Manconi, M. et al., 2007. Intracellular distribution of fluorescent probes delivered by vesicles of different lipidic composition. *Colloids and Surfaces B: Biointerfaces,* p. 143–151.

Marambaud, P., Zhao, H. & Davies, P., 2005. Resveratrol Promotes Clearance of Alzheimer's Disease Amyloid-beta Peptides. *The Journal of Biological Chemistry,* Volume 280, p. 37377–37382.

Marques, O. & Outeiro, T., 2012. Alpha-synuclein: from secretion to dysfunction and death. *Cell Death and Disease,* Volume 3, pp. 1-7.

Mason, J., Kokkoni, N., Stott, K. & Doig, A., 2003. Design strategies for anti-amyloid agents. *Current Opinion in Structural Biology ,* Volume 13, pp. 526-32.

McCammon, D., 2014. Medical Food to Stop the Progression of Parkinson's Disease. *Parkinson's Disease,* Volume 3, pp. 10-13.

Meraz-Ríos, M. et al., 2010. Tau oligomers and aggregation in Alzheimer's disease. *Journal of Neurochemistry,* Volume 112, p. 1353–1367.

Michan, S. & Sinclair, D., 2007. Sirtuins in mammals: insights into their biological function. *Biochemical Journal,* Volume 404, pp. 1-27.

Michishita, E. et al., 2005. Evolutionarily Conserved and Nonconserved Cellular Localizations and Functions of Human SIRT Proteins. *Molecular Biology of the Cell,* Volume 16, p. 4623–4635.

Milne, J. & Denu, J., 2008. The Sirtuin family: therapeutic targets to treat diseases of aging. *Current Opinion in Chemical Biology,* Volume 12, p. 11–17.

Morris, M. et al., 2002. Dietary Intake of Antioxidants Nutrients and Risk of Alzheimer Disease a Biracial Community Study. *Journal of the American Medical Association,* Volume 287, pp. 3230-3237.

Mudshinge, S. R., Deore, A. B., Patil, S. & Bhalgat, C. M., 2011. Nanoparticles: Emerging carriers for drug delivery. *Saudi Pharmaceutical Journal ,* pp. 129-141.

Mufamadi, M. et al., 2010. A Review on Composite Liposomal Technologies for Specialized Drug Delivery. *Journal of Drug Delivery,* pp. 1-19.

Murakami, H., Kobayashi, M., Takeuchi, H. & Kawashima, Y., 1999. Preparation of poly(DL-lactide-co-glycolide) nanoparticles by modified spontaneous emulsification solvent diffusion method. *International Journal of Pharmaceutics,* Volume 187, p. 143–152.

Musumeci, T. et al., 2006. PLA/PLGA nanoparticles for sustained release of docetaxel. *International Journal of Pharmaceutics,* Volume 325, pp. 172-9.

Neves, A. R., Lúcio, M., Lima, J. L. & Reis, S., 2012. Resveratrol in Medicinal Chemistry: A Critical Review of its Pharmacokinetics, Drug-Delivery, and Membrane Interactions. *Current Medicinal Chemistry,* Volume 19, pp. 1663-1681.

Nicolás, J. et al., 2006. Determination of stoichiometric coefficients and apparent formation constants for beta-cyclodextrin complexes of trans-resveratrol using reversed-phase liquid chromatography. *Journal of Chromatography A,* p. 158–165.

Nilsson, M., 2004. Techniques to study amyloid fibril formation in vitro. *Methods,* Volume 34, p. 151–160.

Nilsson, M. R., 2004. Techniques to study amyloid fibril formation in vitro. *Methods,* Volume 34, pp. 151-160.

Niranjan, R., 2014. The Role of inflammatory and oxidative stress mechanisms in the pathogenesis of Parkinson's disease: Focus on astrocytes. *Molecular Neurobiology,* Volume 49, p. 28–38.

Ohtsuki, S. & Terasaki, T., 2007. Contribution of Carrier-Mediated Transport Systems to the Blood–Brain Barrieras a Supporting and Protecting Interface for the Brain; Importance for CNS Drug Discovery and Development. *Pharmaceutical Research,* Volume 24, pp. 1745-1758.

Okawara, M. et al., 2007. Resveratrol protects dopaminergic neurons in midbrain slice culture from multiple insults. *Biochemical Pharmacology,* Volume 73, p. 550–560.

Ono, K. et al., 2008. Effects of Grape Seed-derived Polyphenols on Amyloid beta-Protein Self-assembly and Cytotoxicity. *The Journal of Biological Chemistry,* Volume 283, p. 32176–32187.

Pan, T., Kondo, S., Le, W. & Jankovic, J., 2008a. The role of autophagy-lysosome pathway in neurodegeneration associated with Parkinson's disease. *Brain,* Volume 131, pp. 1969-1978.

Pan, T. et al., 2008b. Neuroprotection of rapamycin in lactacystin-induced neurodegeneration via autophagy enhancement. *Neurobiology of Disease,* Volume 32, p. 16–25.

Pan, T. et al., 2009. Rapamycin protects against rotenone-induced apoptosis through autophagy induction. *Neuroscience,* Volume 164, p. 541–551.

Pardridge, W., 2002. Drug and Gene Delivery to the Brain: The Vascular Route. *Neuron,* Volume 36, p. 555-558.

Pardridge, W., 2002. Why is the global CNS pharmaceutical market so under-penetrated?. *Drug Discovery Today,* Volume 7, pp. 5-7.

Pardridge, W., 2003. Blood-Brain Barrier Drug Targeting: The Future of Brain Drug Development. *Molecular Interventions,* Volume 3, pp. 90-105.

Pardridge, W., 2005. The Blood-Brain Barrier: Bottleneck in Brain Drug Development. *The Journal of the American Society for Experimental NeuroTherapeutics,* Volume 2, pp. 3-14.

Pardridge, W., 2012. Drug transport across the blood–brain barrier. *Journal of Cerebral Blood Flow & Metabolism,* Volume 32, p. 1959–1972.

Parker, A. et al., 2005. Resveratrol rescues mutant polyglutamine cytotoxicity in nematode and mammalian neurons. *Nature Genetics,* Volume 37, pp. 349-350.

Patel, K. et al., 2011. Clinical trials of resveratrol. *Annals of the new york academy of sciences,* p. 161–169.

Perfeito, R. & Rego, A., 2011. Role of alpha-synuclein and Parkinson's disease-associated mitochondrial dysfunction. *Review Neuroscience,* pp. 1-12.

Pimentel, M. F., Neto, B. B., Saldanha, T. C. & Araújo, M. C., 1998. Effects of experimental design on calibration curve precision in routine analysis. *Journal of Automatic Chemistry,* Volume 20, pp. 9-15.

Popovska, O., Simonovska, J., Kavrakovski, Z. & Rafajlovska, V., 2013. An Overview: Methods for Preparation and Characterization of Liposomes as Drug Delivery Systems. *International Journal of Pharmaceutical and Phytopharmacological Research,* Volume 3, pp. 13-20.

Pringsheim, T., Jette, N., Frolkis, A. & Steeves, T., 2014. The Prevalence of Parkinson's Disease: A Systematic Review and Meta-analysis. *Movement Disorders,* Volume 29, pp. 1583-1590.

Prokop, A. & Davidson, J. M., 2013. Nanovehicular Intracellular Delivery Systems. *Journal of Pharmaceutical Sciences,* pp. 1-100.

Qiang, L., Wang, H. & Farmer, S., 2007. Adiponectin Secretion Is Regulated by SIRT1 and the Endoplasmic Reticulum Oxidoreductase Ero1-L. *Molecular and Cellular Biology,* Volume 27, p. 4698–4707.

Qin, W. et al., 2006. Neuronal SIRT1 Activation as a Novel Mechanism Underlying the Prevention of Alzheimer Disease Amyloid Neuropathology by Calorie Restriction. *The Journal of Biological Chemistry,* Volume 281, pp. 21745-21754.

Ramos-Cabrer, P. & Campos, F., 2013. Liposomes and nanotechnology in drug development: focus on neurological targets. *International Journal of Nanomedicine,* Volume 8, p. 951–960.

Reitz, C., 2012. Alzheimer's Disease and the Amyloid Cascade Hypothesis: A Critical Review. *International Journal of Alzheimer's Disease,* pp. 1-12.

Rivière, C. et al., 2007. Inhibitory activity of stilbenes on Alzheimer's beta-amyloid fibrils in vitro. *Bioorganic & Medicinal Chemistry,* Volume 15, p. 1160–1167.

Robb, E., Page, M., Wiens, B. & Stuart, J., 2008. Molecular mechanisms of oxidative stress resistance induced by resveratrol: Specific and progressive induction of MnSOD. *Biochemical and Biophysical Research Communications,* Volume 367, p. 406–412.

Rocha, F. & Teixeira, L., 2004. Estratégias para aumento de sensibilidade em espectrofotometria UV-VIS. *Química Nova,* Volume 5, pp. 807-812.

Rocha, S. et al., 2009. Design and biological activity of beta-sheet breaker peptide conjugates. *Biochemical and Biophysical Research Communications,* Volume 380, p. 397–401.

Rodgers, J. & Puigserver, P., 2007. Fasting-dependent glucose and lipid metabolic response through hepatic sirtuin 1. *Proceedings of the National Academy of Sciences,* Volume 104, p. 12861–12866.

Sabaté, R. & Estelrich, J., 2005. Stimulatory and Inhibitory Effects of Alkyl Bromide Surfactants on beta-Amyloid Fibrillogenesis. *Langmuir,* Volume 21, pp. 6944-6949.

Sabate, R. et al., 2013. Thioflavin-T excimer formation upon interaction with amyloid fibers. *Chemical Communications,* Volume 49, pp. 5745--5747.

Saiko, P., Szakmary, A., Jaeger, W. & Szekeres, T., 2008. Resveratrol and its analogs: Defense against cancer, coronary disease and neurodegenerative maladies or just a fad?. *Mutation Research,* Volume 658, p. 68–94.

Salon, L. et al., 2000. Defective Ubiquitination of Cerebral Proteins in Alzheimer's Disease. *Journal of Neuroscience Research,* Volume 62, p. 302–310.

Salvati, E. et al., 2013. Liposomes functionalized to overcome the blood–brain barrier and to target amyloid-β peptide: the chemical design affects the permeability across an in vitro model. *International Journal of Nanomedicine,* Volume 8, p. 1749–1758.

Santos, F. M., Crotti, A. M. & Cunha, W. R., n.d. *Aplicação da técnica CLAE-DAD-EM/EM na identificação de flavonóides de Tibouchina candolleana (Melastomataceae).* s.l.:s.n.

Schapira, A., 2008. Mitochondria in the aetiology and pathogenesis of Parkinson's disease. *The Lancet Neurology,* Volume 7, p. 97–109.

Schnyder, A. & Huwyler, J., 2005. Drug Transport to Brain with Targeted Liposomes. *The Journal of the American Society for Experimental NeuroTherapeutics,* Volume 2, p. 99 –107.

Schubert, S., Delaney, J. T. & Schubert, U. S., 2011. Nanoprecipitation and nanoformulation of polymers: from history to powerful possibilities beyond poly(lactic acid). *The Royal Society of Chemistry,* Volume 7, p. 1581–1588.

Selkoe, D., 2001. Alzheimer's Disease: Genes, Proteins, and Therapy. *Alzheimer's Disease,* Volume 81, pp. 741-766.

Selkoe, D., 2001. Presenilins, b-amyloid precursor protein and the molecular basis of Alzheimer's disease. *Clinical Neuroscience Research,* pp. 91-103.

Selvaraj, S. et al., 2013. Dose-Dependent Interaction of trans-Resveratrol with Biomembranes: Effects on Antioxidant Property. *Journal of Medicinal Chemistry,* Volume 56, p. 970–981.

Shashi, K., Satinder, K. & Bharat, P., 2012. A complete review on: lipossomes. *International Research Journal of Pharmacy,* pp. 10-16.

Shi, T., Wang, F., Stieren, E. & Tong, Q., 2005. SIRT3, a Mitochondrial Sirtuin Deacetylase, Regulates Mitochondrial Function and Thermogenesis in Brown Adipocytes. *The Journal of Biological Chemistry,* Volume 280, p. 13560 –13567.

Sirisha, V. et al., 2012. Liposomes – the potential drug carriers. *Journal of Pharmacy,* Volume 2, pp. 26-38.

Small, S. & Duff, K., 2008. Linking Ab and Tau in Late-Onset Alzheimer's Disease: A Dual Pathway Hypothesis. *Neuron,* pp. 534-542.

Sommer, B., 2002. Alzheimer's disease and the amyloid cascade hypothesis: ten years on. *Neurosciences,* Volume 2, p. 87–92.

So, P. & Dong, C., 2002. Fluorescence Spectrophotometry. *Encyclopedia of life sciences,* pp. 1-4.

Soto, C. et al., 1995. Fibrillogenesis of synthetic amyloid-beta peptides is dependent on their initial secondary structure. *Neuroscience Letter,* Volume 200, pp. 105-108.

Souza, C. et al., 2011. Parkinson's disease and the Process of Aging Motor: Literature Review. *Review of Neuroscience,* Volume 19, pp. 718-723.

Stefanis, L., 2012. Alpha-Synuclein in Parkinson's Disease. *Cold Spring Harbor Perspectives in Medicine,* pp. 1-23.

Sun, A., Wang, Q., Simonyi, A. & Sun, G., 2010. Resveratrol as a Therapeutic Agent for Neurodegenerative Diseases. *Molecular Neurobiology,* Volume 41, p. 375–383.

Sun, B. et al., 2006. Stilbenes: Quantitative extraction from grape skins, contribution of grape solids to wine and variation during wine maturation. *Analytica Chimica Acta,* Volume 563, pp. 382-390.

Sun, X., Peng, B. & Yan, W., 2008. Measurement and correlation of solubility of trans-resveratrol in 11 solvents at T = (278.2, 288.2, 298.2, 308.2, and 318.2) K. *The Journal of Chemical Thermodynamics,* Volume 40, p. 735–738.

Tambosco, L. et al., 2014. Effort training in Parkinson's disease: A systematic review. *Annals of Physical and Rehabilitation Medicine,* Volume 57, p. 79–104.

Thomas, B. & Beal, F., 2007. Parkinson's disease. *Human Molecular Genetics,* Volume 16, p. R183–R194.

Thomas, B. & Beal, F., 2007. Parkinson's disease. *Human Molecular Genetics,* Volume 16, p. R183–R194.

Torchelin, V. et al., 1994. poly(ethylene glycol) on the liposome surface: on the mechanism of polymer-coated liposome longevity. *Biochimica et Biophysica Acta ,* Volume 1195, pp. 11-20.

Torchilin, V., 2005. Recent Advances With Liposomes as Pharmaceutical Carriers. *Drug Discovery,* Volume 4, pp. 145-160.

Trela, B. C. & Waterhouse, A. L., 1996. Resveratrol: Isomeric Molar Absorptivities and Stability. *Journal of Agricultural and Food Chemistry ,* Volume 44, pp. 1253-1257.

Trump, D. L., Deeb, K. K. & Johnson, C. S., 2010. Vitamin D: considerations in the continued development as an agent for cancer prevention and therapy. *The Cancer Journal,* Volume 16, pp. 1-9.

Upadhyay, R., 2014. Drug Delivery Systems, CNS Protection, and the Blood Brain Barrier. *BioMed Research International,* pp. 1-37.

Vanaja, K., Wahl, M., Bukarica, L. & Heinle, H., 2013. Liposomes as carriers of the lipid soluble antioxidant resveratrol: Evaluation of amelioration of oxidative stress by additional antioxidant vitamin. *Life Sciences,* Volume 93, p. 917–923.

Vasir, J. K. & Labhasetwar, V., 2007. Biodegradable Nanoparticles for Cytosolic Delivery of Therapeutics. *Advanced Drug Delivery Reviews,* Volume 59, p. 718–728.

Vian, M. et al., 2005. Simple and rapid method for cis- and trans-resveratrol and piceid isomers determination in wine by high-performance liquid chromatography using Chromolith columns. *Journal of Chromatography A,* p. 224–229.

Walle, T., 2011. Bioavailability of resveratrol. *Annals of the New York academy of sciences,* p. 9–15.

Wang, C. et al., 2006. Interactions between E2F1 and SirT1 regulate apoptotic response to DNA damage. *Nature Cell Biology,* Volume 8, pp. 1025-1031.

Wang, Z., Chui, W. K. & Ho, P. C., 2009. Design of a multifunctional PLGA nanoparticulate drug delivery system: evaluation of its physicochemical properties and anticancer activity to malignant cancer cells. *Pharmaceutical Research,* Volume 26, pp. 1162-71.

Wang, Z. L., 2000. Transmission Electron Microscopy of Shape-Controlled Nanocrystals and Their Assemblies. *The Journal of Physical Chemistry B,* Volume 104, pp. 1153-1175.

Wilczewska, A. Z., Niemirowicz, K., Markiewicz, K. H. & Car, H., 2012. Nanoparticles as drug delivery systems. *Pharmacological Reports,* Volume 64, pp. 1020-1030.

Winklhofer, K. & Haass, C., 2010. Mitochondrial Dysfunction in Parkinson's Disease. *Biochimica et Biophysica Acta,* Volume 1802, pp. 29-44.

Wischke, C. & Schwendeman, S. P., 2008. Principles of encapsulating hydrophobic drugs inPLA/PLGA microparticles. *International Journal of Pharmaceutics,* Volume 364, pp. 298-327.

Wohlfart, S., Gelperina, S. & Kreuter, J., 2012. Transport of drugs across the blood–brain barrier by nanoparticles. *Journal of Controlled Release,* Volume 16, p. 264–273.

Wolpin, B. et al., 2012. Plasma 25-hydroxyvitamin D and risk of pancreatic cancer. *Cancer Epidemiology, Biomarkers & Prevention,* Volume 21, pp. 82-91.

Wu, Y. et al., 2011. Resveratrol-Activated AMPK/SIRT1/Autophagy in Cellular Models of Parkinson's Disease. *Neurosignals,* Volume 19, p. 163–174.

Xiong, S. et al., 2013. Size influences the cytotoxicity of poly (lactic-co-glycolic acid) (PLGA) and titanium dioxide (TiO2) nanoparticles. *Archives of Toxicology,* Volume 87, pp. 1075-86.

Zatta, P., Drago, D., Bolognin, S. & Sensi, S., 2009. Alzheimer's disease, metal ions and metal homeostatic therapy. *Pharmacological Sciences,* Volume 30, pp. 346-355.

Zhang, L. et al., 2008. Nanoparticles in Medicine: Therapeutic Applications and Developments. *Clinical Pharmacology and Therapeutics,* Volume 83, pp. 761-769.

Zhang, W. et al., 2005. Aggregated alpha-synuclein activates microglia: a process leading to disease progression in Parkinson's disease. *Federation of American Societies for Experimental Biology,* Volume 19, pp. 533-542.

Zivadinov, R. et al., 2003. A longitudinal study of quality of life and side effects in patients with multiple sclerosis treated with interferon beta-1a. *Journal of the Neurological Sciences,* Volume 216, p. 113 – 118.

Zupančič, Š., Lavrič, Z. & Kristl, J., 2015. Stability and solubility of trans-resveratrol are strongly influenced by ph and temperature. *European Journal of Pharmaceutics and Biopharmaceutics Maceutics.*